Haptic Sensors and Interfaces

Emil M. Petriu, Dr. Eng., FIEEE
School of Electrical Engineering and Computer Science
University of Ottawa, Canada
http://www.site.uottawa.ca/~petriu

Human Haptic Perception

Human haptic perception is the result of a complex dexterous manipulation act involving two distinct components:

(i) ***cutaneous*** information from touch sensors which provide about the geometric shape, contact force, elasticity, texture, and temperature of the touched object area. The highest density of cutaneous sensors is found in fingerpads (but also in the tongue, the lips, and the foot). Force information is mostly provided by sensors on muscles, tendons and bone joints proprioceptors;

(ii) ***kinesthetic*** information about the positions and velocities of the kinematic structure (bones and muscles) of the hand

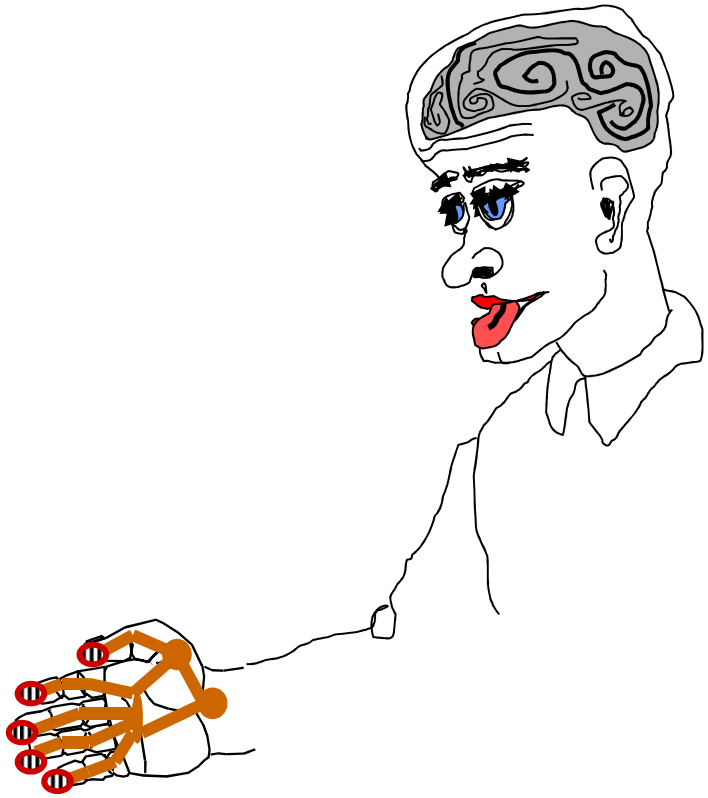

Human Haptic Perception

Human haptic perception is the result of a complex dexterous manipulation act involving two distinct components:

(i) ***cutaneous*** information from touch sensors which provide about the geometric shape, contact force, elasticity, texture, and temperature of the touched object area. The highest density of cutaneous sensors is found in fingerpads (but also in the tongue, the lips, and the foot). Force information is mostly provided by sensors on muscles, tendons and bone joints proprioceptors;

(ii) ***kinesthetic*** information about the positions and velocities of the kinematic structure (bones and muscles) of the hand

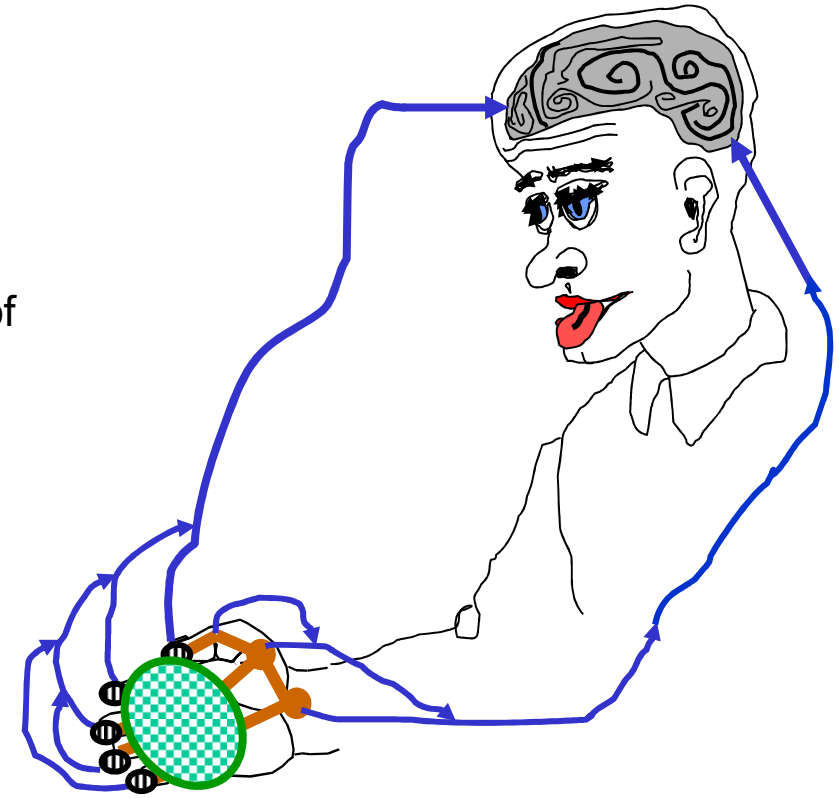

“In a way, touch can be constructed as the most reliable of the [human] sensor modalities. When the senses conflict, touch is usually the ultimate arbiter. … Touch sensations can arise from stimulation anywhere on the body’s surface. Indeed, the **skin can be characterized as one large receptor surface for the sense of touch**. … The English neurologist H. Jackson paid homage to the wonderful and complex abilities of the *human hand* by calling it *the most intelligent part of the body*. The skin on the human hand contains thousands of **mechanoreceptors** (sensitive to mechanical pressure of deformation of the skin), as well as a **complex set of muscle to guide the fingers** as they explore the surface of an object. The mechanoreceptors play a key role in analyzing object detail such as texture; the muscles make their big contribution when grosser features such as size, weight, and shape are being analyzed. But, whether exploring gross or small details, the **hand and the finger pads convey the most useful tactile information about objects**. In this respect, the hand is analogous to the eye’s fovea, the region of retina associated with keen visual acuity. There is, however, a flaw in this analogy: fovea vision is most acute when the eye is relatively stationary, but **touch acuity is best when the fingers move of the object of regard** ” (from [R. Sekuler, R. Balke, *Perception*, 2nd edition, McGraw-Hill, NY, 1990, Chapter 11. Touch, pp. 357-383]).

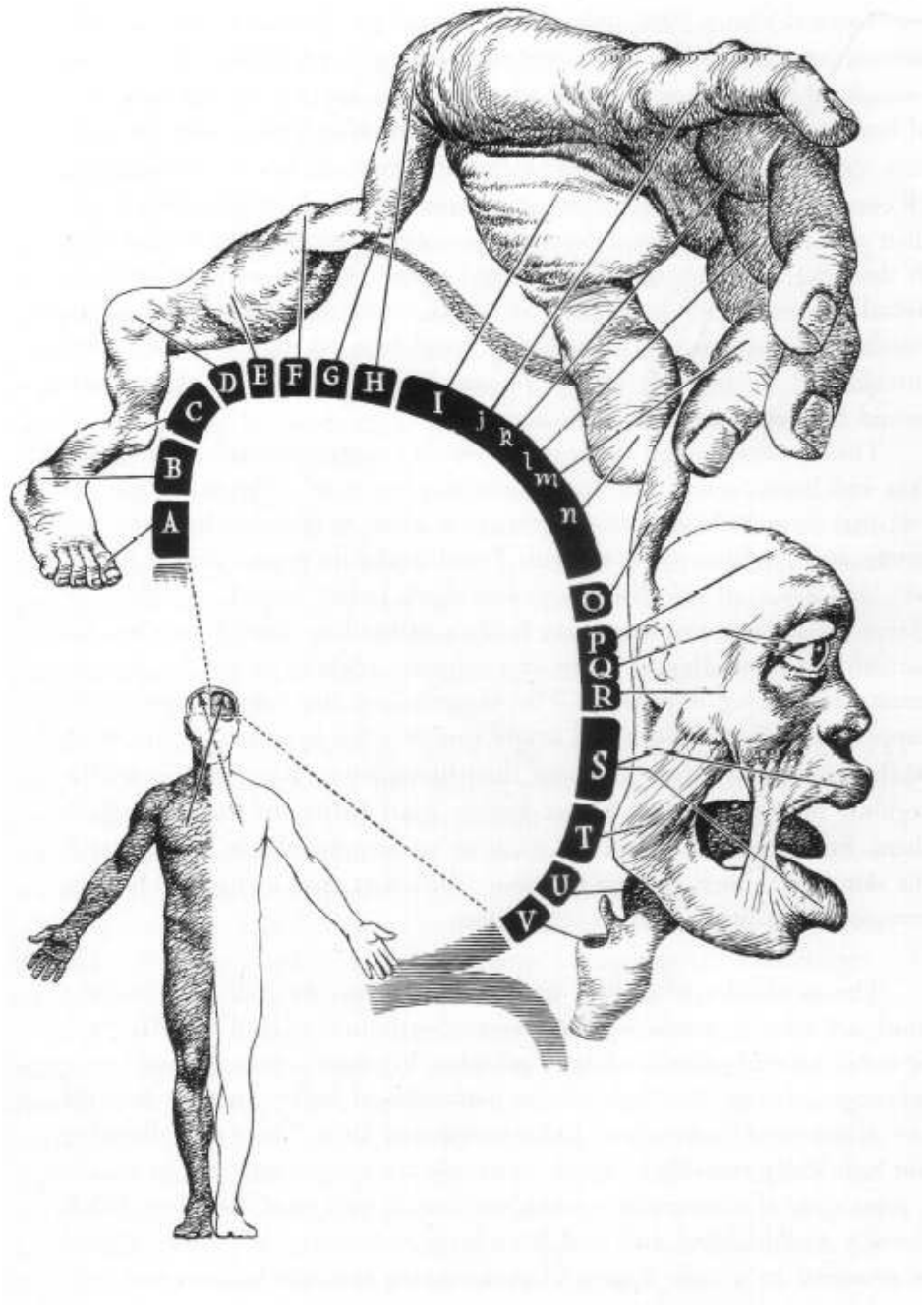

The sensory cortex: an oblique strip, on the side of each hemisphere, receives sensations from parts on the opposite side of the body and head: foot (A), leg (B, C, hip (D), trunk (E), shoulder (F), arm (G, H), **hand (I, J, K, L, M, N),** neck (O), cranium (P), eye (Q), temple (R), lips (S), cheek (T), tongue (U), and larynx (V). Highly sensitive parts of the body, such as the hand, lips, and tongue have proportionally large mapping areas, the foot, leg, hip, shoulder, arm, eye, cheek, and larynx have intermediate sized mapping areas, while the trunk, neck, cranium, and temple have smaller mapping areas.
(from [H. Chandler Elliott, *The Shape of Intelligence - The Evolution of the Human Brain*, Drawings by A. Ravielli, Charles Scribner's Sons, NY, 1969])

Cutaneous Sensing

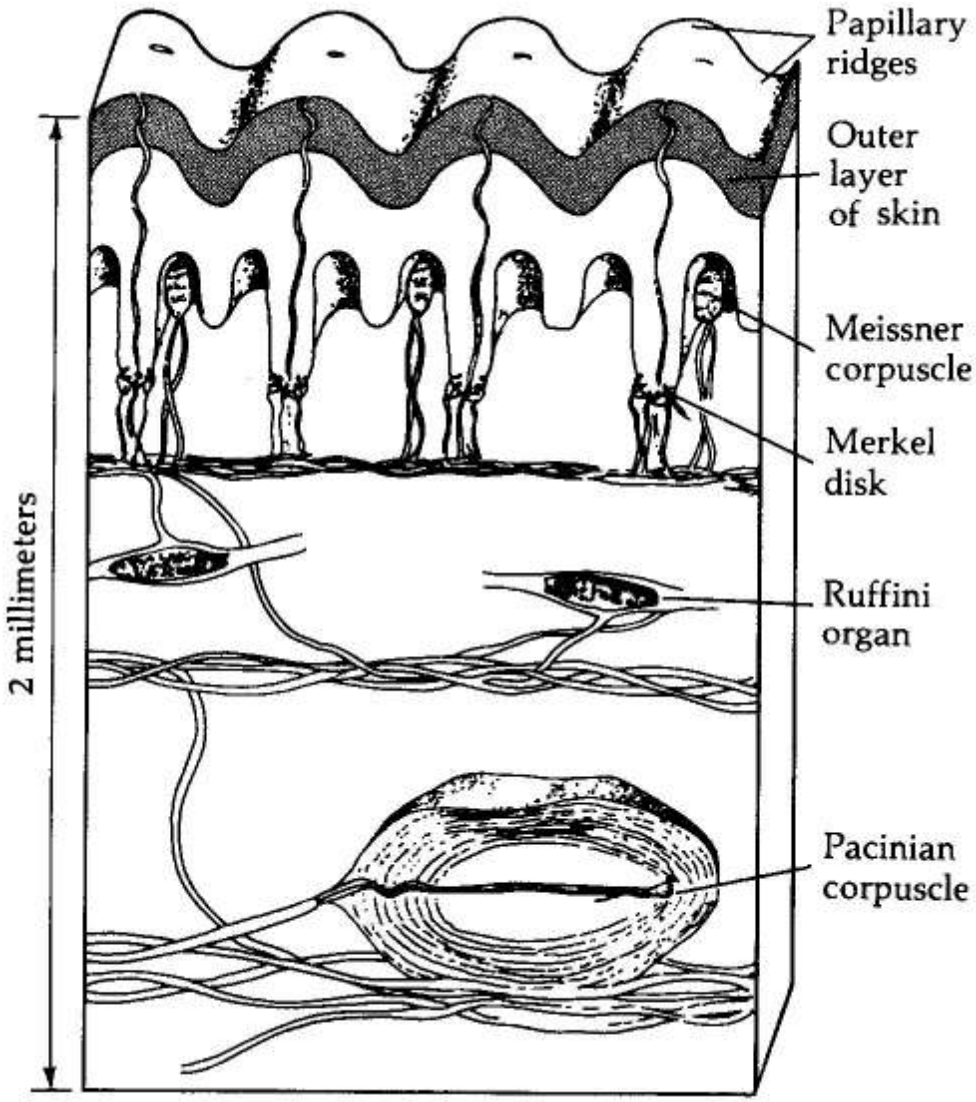

Cutaneous sensors:

The highest density of cutaneous sensors is found in fingertips, but also in the foot soles, the tongue, and the lips.

Force information is mostly provided by sensors on muscle tendons and bones/joints proprioceptors;

Cross section through the skin of primate finger pad showing the location of specialized nerve fiber terminals (from [R. Sekuler, R. Balke, *Perception*, 2nd edition, McGraw-Hill, NY, 1990]).

[Burdea& Coiffet 2003] G. Burdea and Ph. Coiffet, Virtual Reality Technology, (2nd edition), Wiley, New Jersey, 2003

Cutaneous sensors =>

- 40 % are *Meissner's corpuscles* sensing velocity and providing information about the movement across the skin;
- 25% are *Merkel's disks* which measure pressure and vibrations;
- 13 % are *Pacinian corpuscles* (buried deeper in the skin) sensing acceleration and vibrations of about 250 Hz;
- 19% are *Rufini corpuscles* sensing skin shear and temperature changes.

[Burdea& Coiffet 2003] Comparison of various skin mechanoreceptorss

Receptor Type	Rate of Adaptation	Stimulus frequency (Hz)	Receptive Field	Function
Merkel Disks	SA-I	0–10	Small, well defined	Edges, intensity
Ruffini Corpuscles	SA-II	0–10	Large, indistinct	Static force, skin stretch
Meissner Corpuscles	FA-I	20–50	Small, well defined	Velocity, edges
Pacinian Corpuscles	FA-II	100–300	Large, indistinct	Acceleration, vibration

Based on Seow [1988], Cholewiak and Collins [1991], and Kalawsky [1993]

Spatial resolution
[Burdea& Coiffet 2003]

- If the sensor has a large receptive field – it has
  low spatial resolution
  (Pacinian and Ruffini)
- If the receptive field small - it has high spatial resolution (Meissner and Merkel)

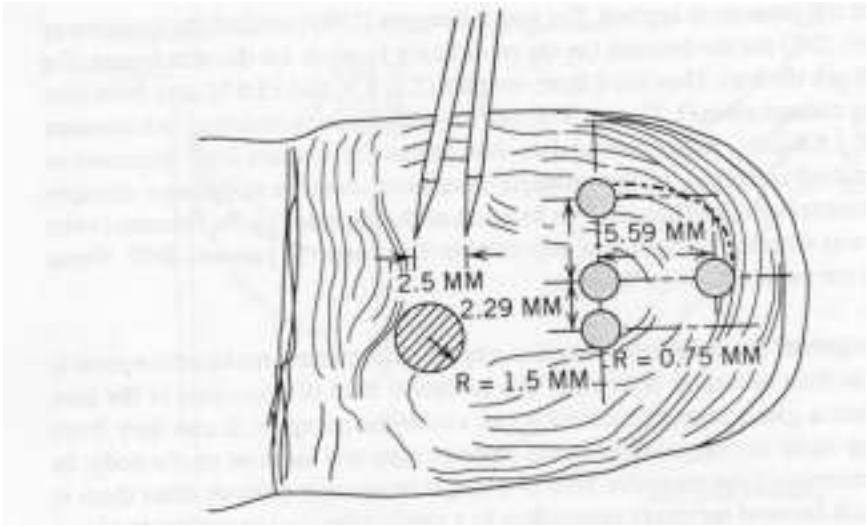

Two-point limen test: 2.5 mm fingertip, 11 mm for palm, 67 mm for thigh (*from [Burdea& Coiffet 2003]*).

Sensor Enabled Robotic Telemanipulation

Robotic dexterous manipulation is an object-oriented act which requires not only specialized *robotic hands with articulated fingers* but also *tactile, force and kinesthetic sensors* for the precise control of the forces and motions exerted on the manipulated object.
As fully autonomous robotic dexterous manipulation is impractical in changing and unstructured environments, an alternative approach is to *combine the low-level robot computer control with the higher-level perception and task planning abilities of a human operator* equipped with adequate *human computer interfaces* (HCI).

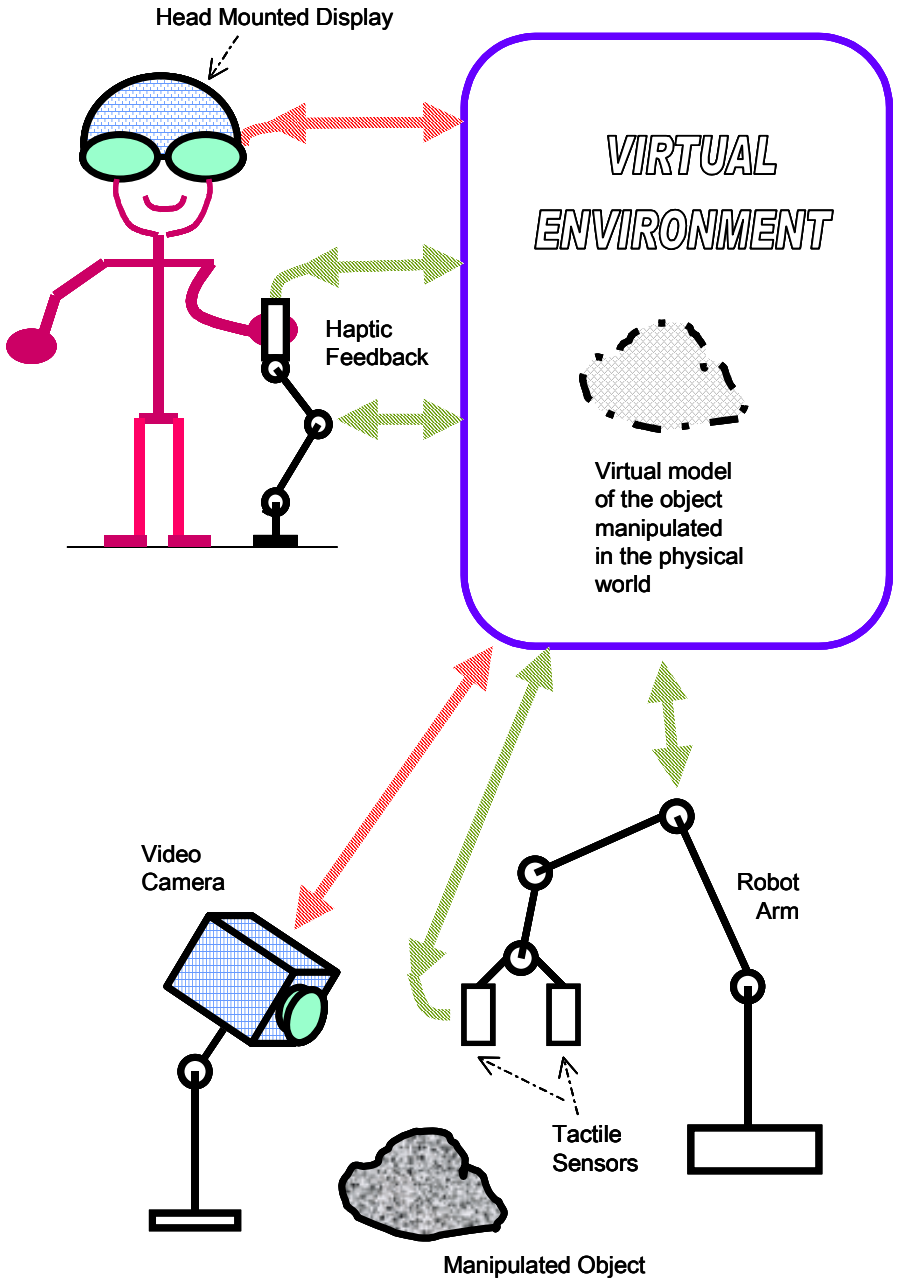

- Telemanipulation systems should have a bilateral architecture that allows a *human operator* to *connect in a transparent manner to a remote robotic manipulator*.

- *Human Computer Interfaces* (HCI) should provide easily perceivable and *task-related sensory displays (monitors) which fit naturally* the perception capabilities of the human operator.

- The potential of the emergent haptic perception technologies is significant for *applications* requiring object telemanipulation such as: (i) robot-assisted handling of materials in industry, hazardous environments, high risk security operations, or difficult to reach environments, (ii) telelearning in hands-on virtual laboratory environments for science and arts, (iii) telemedicine and medical training simulators.

Robot Haptic Sensors

Haptic perception is the result of an active deliberate contact exploratory sensing act.

A **tactile probe** provides the local “cutaneous” information about the touched area of the object.

A **robotic carrier** providing the “kinesthetic” capability is used to move the tactile probe around on the explored object surface and to provide the contact force needed for the probe to extract the desired cutaneous information (e.g. local 3D geometric shape, elastic properties, and/or termic impedance) of the touched object area .

The local *information provided by the tactile probe is integrated with the kinesthetic position parameters of the carrier* resulting in a *composite* **haptic model** (global geometric and elastic profiles, termic impedance map) of the explored 3D object.

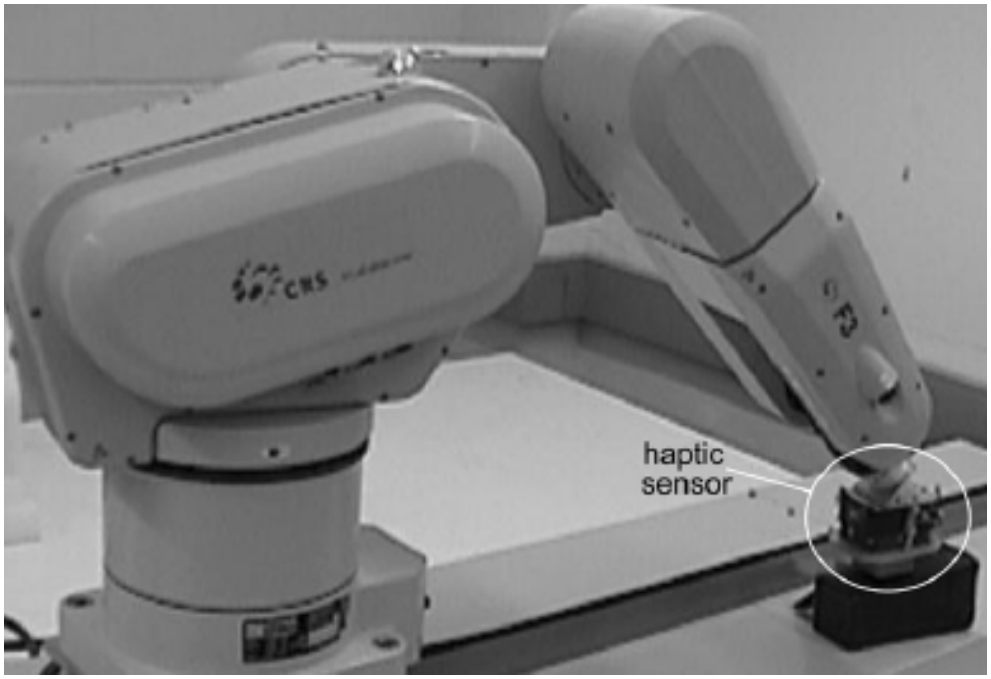

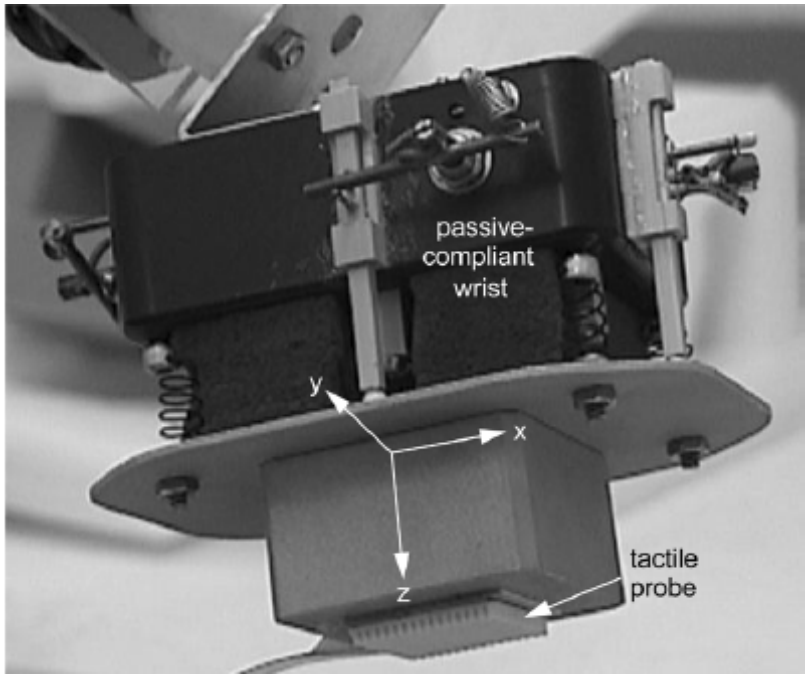

Biology-inspired robot haptic perception system consists of a **robot "finger",** an instrumented **passive-compliant wrist** and a **tactile probe** array. Position sensors placed in the robot joints and on the instrumented passive-compliant wrist provide the kinesthetic information. The compliant wrist allows the probe to accommodate the constraints of the touched object surface and thus to increase the local cutaneous information extracted during the active exploration process under the force provided by the robot.
(from [E.M. Petriu, W.S. McMath, S.K. Yeung, N. Trif, "Active Tactile Perception of Object Surface Geometric Profiles," *IEEE Trans. Instrum. Meas.,* Vol. 41, No. 1, pp.87-92, 1992.]).

Tactile probe for rigid object inspection.

It consists of a force sensitive transducer and an elastic overlay that provides a *geometric profile-to-force* transduction function .

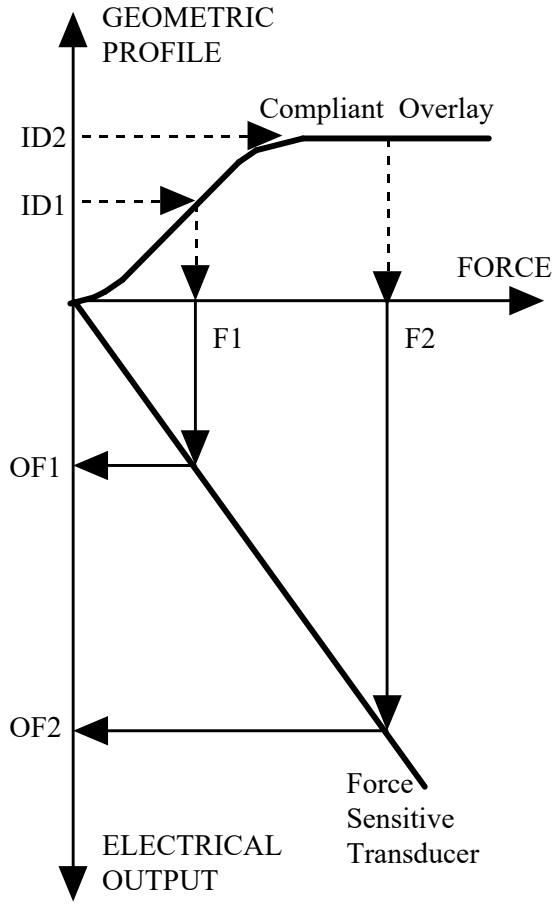

The tactile probe is based on a 16-by-16 matrix of **Force Sensing Resistor (FSR)** elements spaced 1.58 mm apart on a 6.5 cm2 (1 sq. inch) area.

The FSR elements have an exponentially decreasing electrical resistance with applied normal force: the resistance changes by two orders of magnitude over a pressure range of 1 N/cm2 to 100 N/cm2.

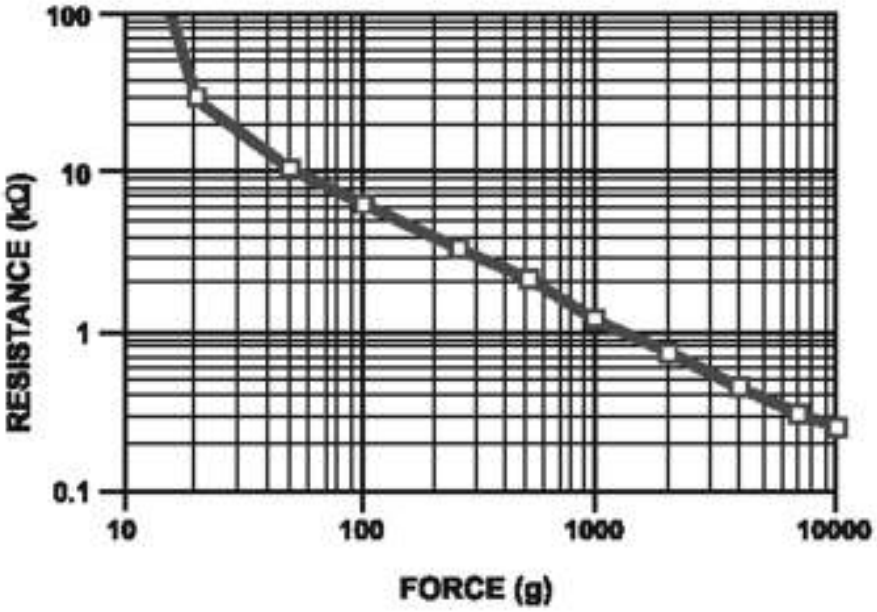

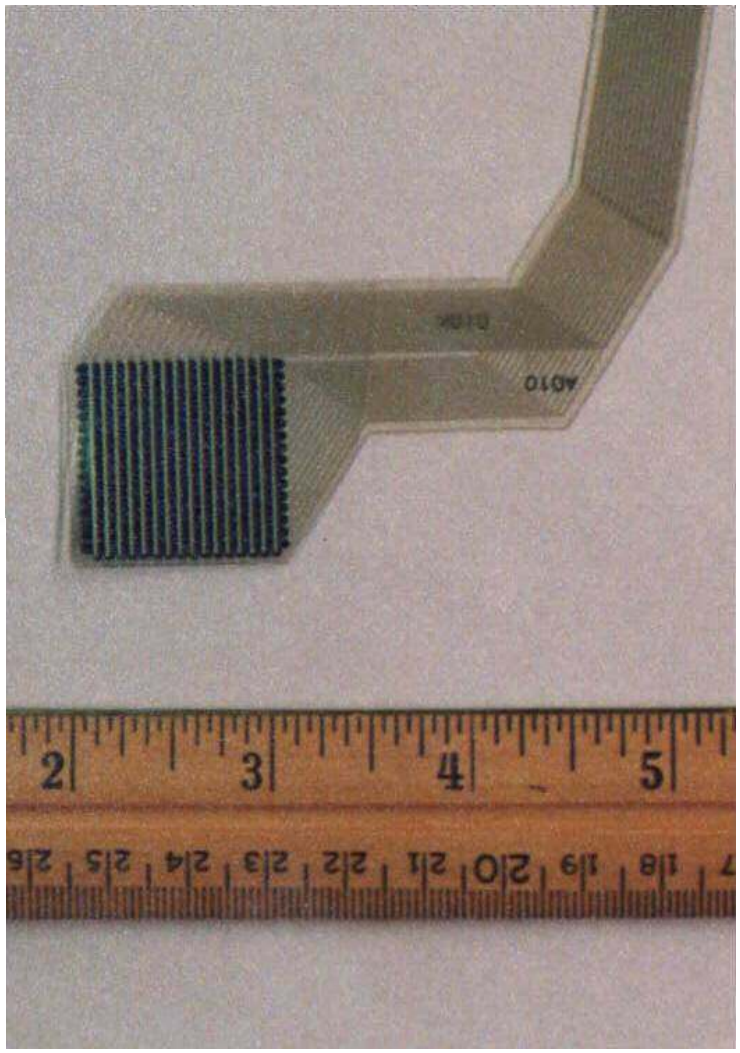

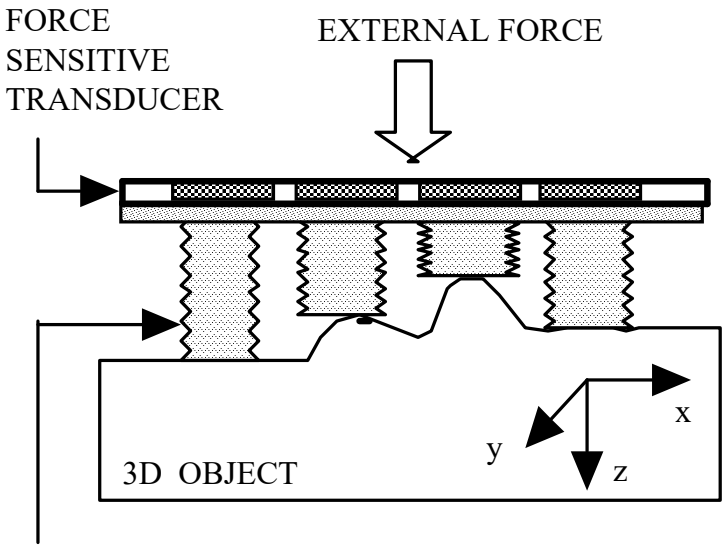

2D- SAMPLING ELASTIC OVERLAY

The ***elastic overlay*** has a protective damping effect against impulsive contact forces and its elasticity resets the transducer when the probe ceases to touch the object.

The crosstalk effect present in one piece elastic pads produces considerable blurring distortions. It is possible to reduce this by using a *custom-designed elastic overlay* consisting of a relatively thin membrane with protruding round tabs. This construction allows free space for the material to expand in the *x* and *y* directions allowing for a compression in the *z* direction proportional with the stress component along this axis.

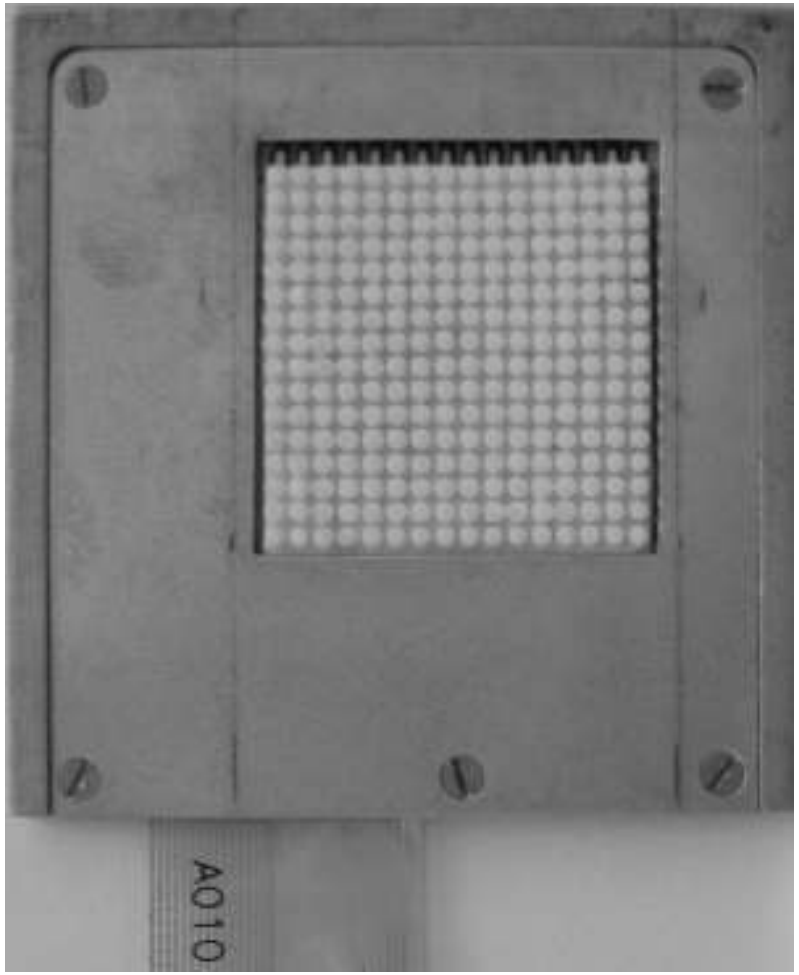

The tabs of the elastic overlay are arranged in a 16-by-16 array having a tab on top of each node of the *FSR* matrix.

This tab configuration provides a *de facto* spatial sampling, which reduces the elastic overlay's blurring effect on the high 2D sampling resolution of the *FSR* transducer.

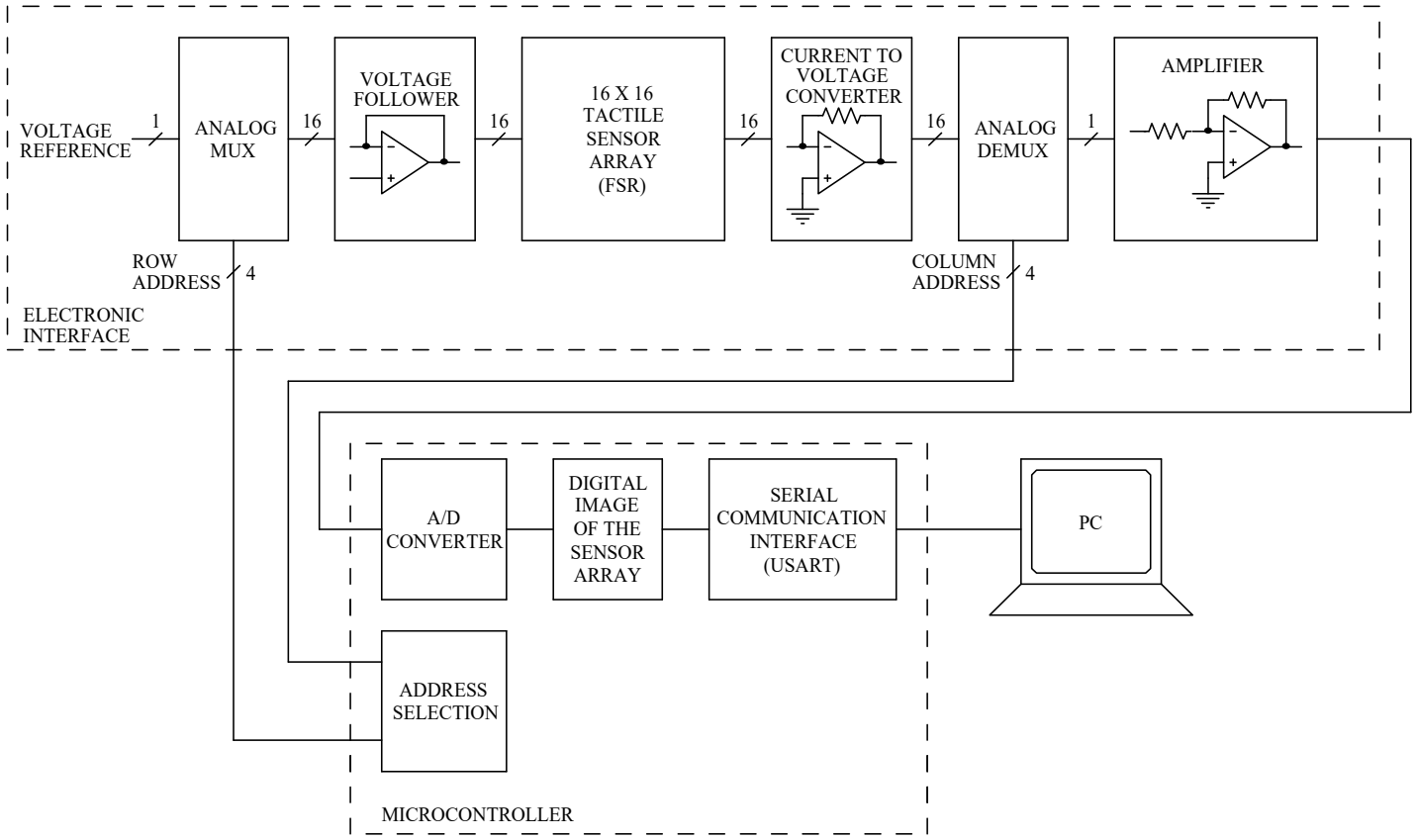

Block-diagram of the tactile sensor interface (from [C. Pasca, *Smart Tactile Sensor*, M.A.Sc. Thesis, University of Ottawa, 2004])

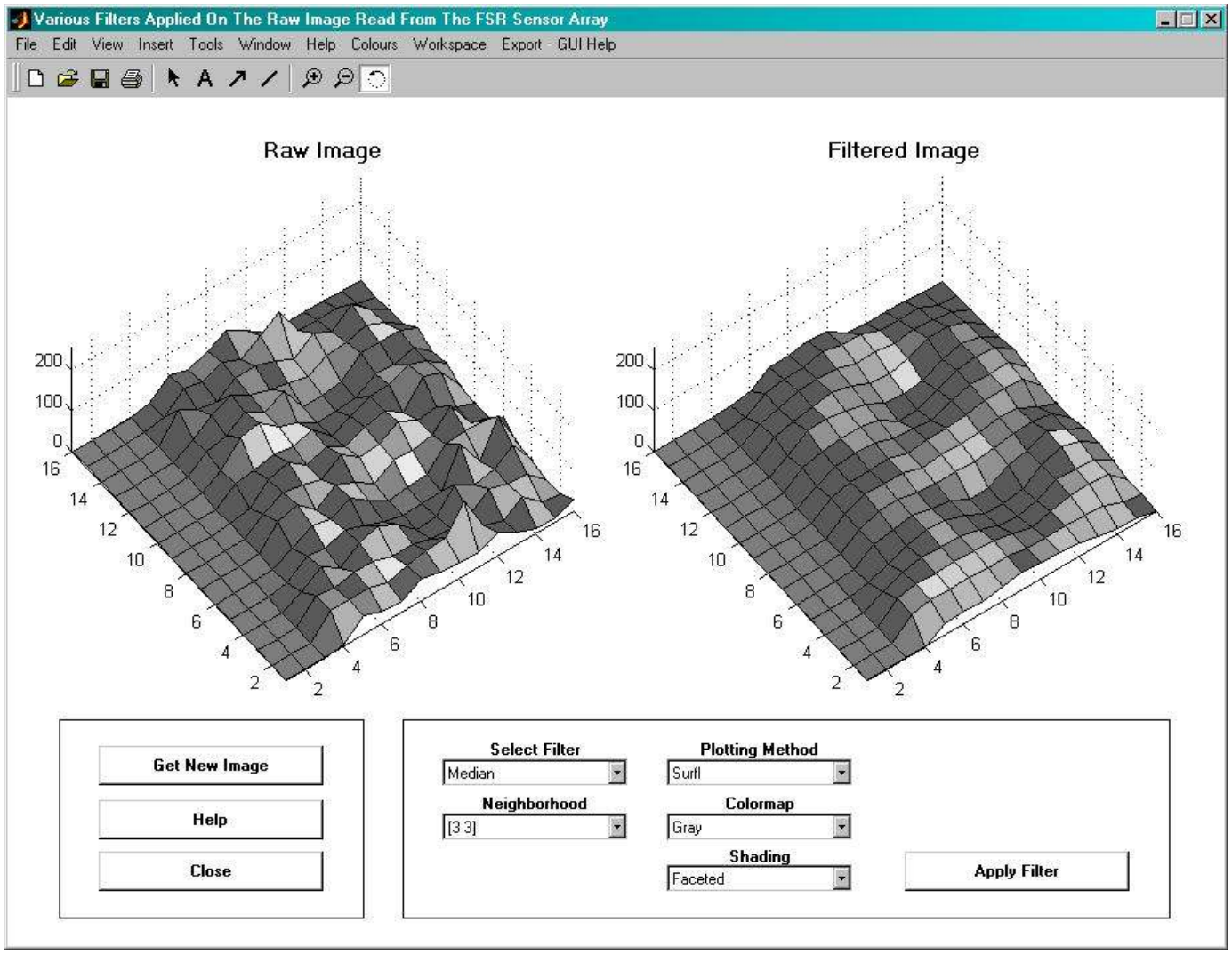

Example of GUI window (from [C. Pasca, *Smart Tactile Sensor*, M.A.Sc. Thesis, University of Ottawa, 2004])

Tactile probe for elastic object inspection.

Recovery of the elastic material properties requires touching each point of interest on the explored object surface and then conducting a strain-stress relation measurement on each of the touched points.

The elastic behaviour at any given point (x_p, y_p, z_p) on the object surface is described by the Hooke's law:

$$\begin{cases} \sigma_p = E_p \cdot \varepsilon_p & if\ 0 \le \varepsilon_p \le \varepsilon_{p\,\max} \\ \sigma_p = \sigma_{p\,\max} & if\ \varepsilon_{p\,\max} < \varepsilon_p \end{cases}$$

where E_p is the modulus of elasticity , s_p is the stress, and e_p is the strain on the normal direction.

Tactile probe for elastic objects: forces with progressively increasing magnitudes are applied on the sampling points using a **contact probe** attached to a **force/torque sensor** and a range profile is collected with the **laser range finder** for each force magnitude.

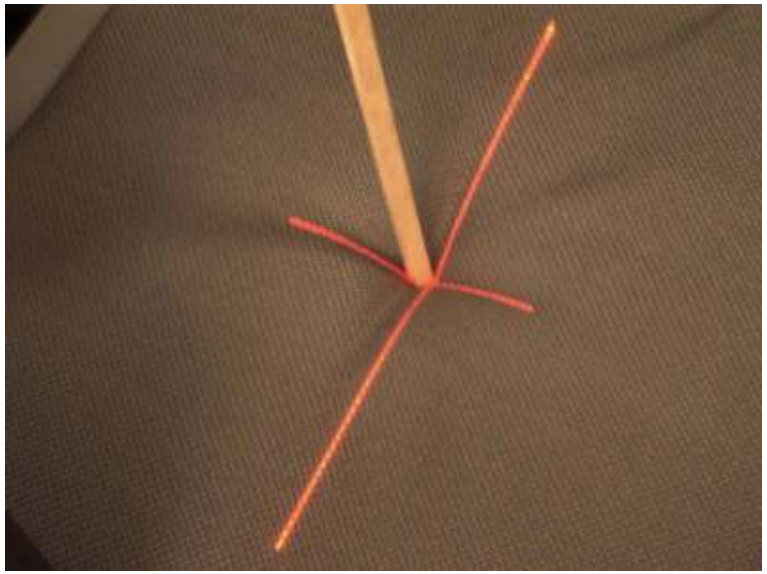

Laser range-finder based recovery of the geometric profiles in an area around the contact point between the probing rod and the object.

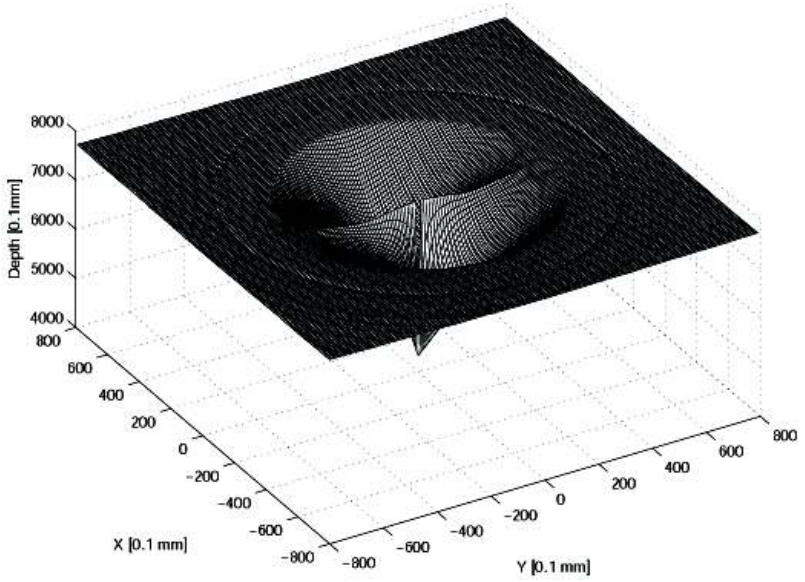

Surface map of the deformation resulting from the force applied by the probing rod.

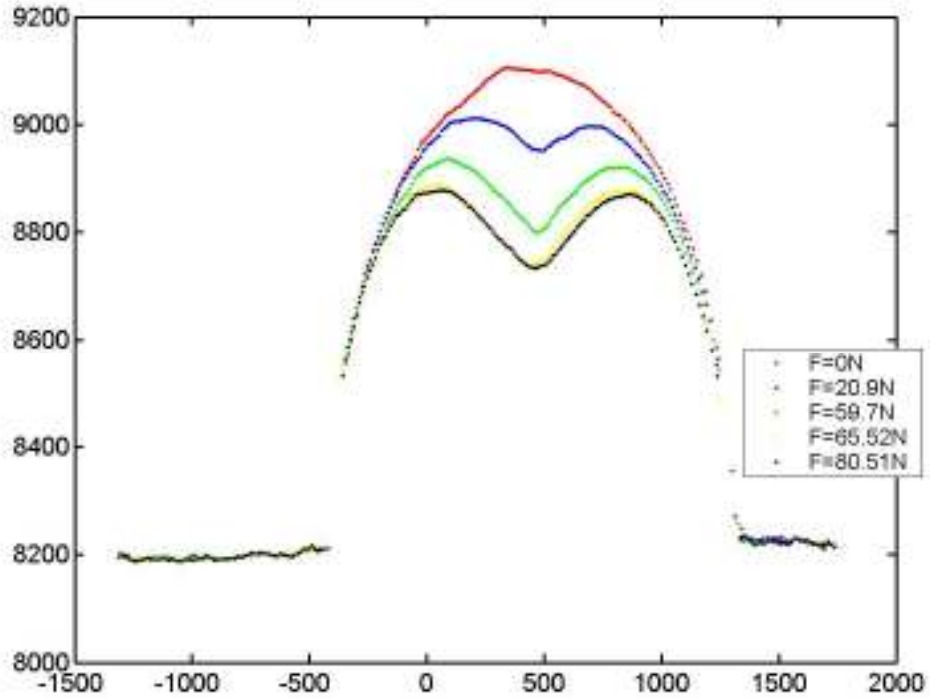

Deformation profiles for rubber for increasing normal force (from .A.M. Cretu, E.M. Petriu, P.Payeur “Neural Network Mapping and Clustering of Elastic Behavior from Tactile and Range Imaging for Virtualized Reality Applications,” submitted to *IEEE Tr. Instr. Meas.,* Nov. 2006).

Haptic Human Interfaces

- These interfaces should allow the human operator to experience natural-like, *conformal to the reality*, feeling of geometric profile, force, texture, elasticity temperature, etc.
- These interfaces should have easily perceivable and *sensor-transparent information displays* (monitors) in such a way to offer a 1:1 mapping of the corresponding human sensory medium.

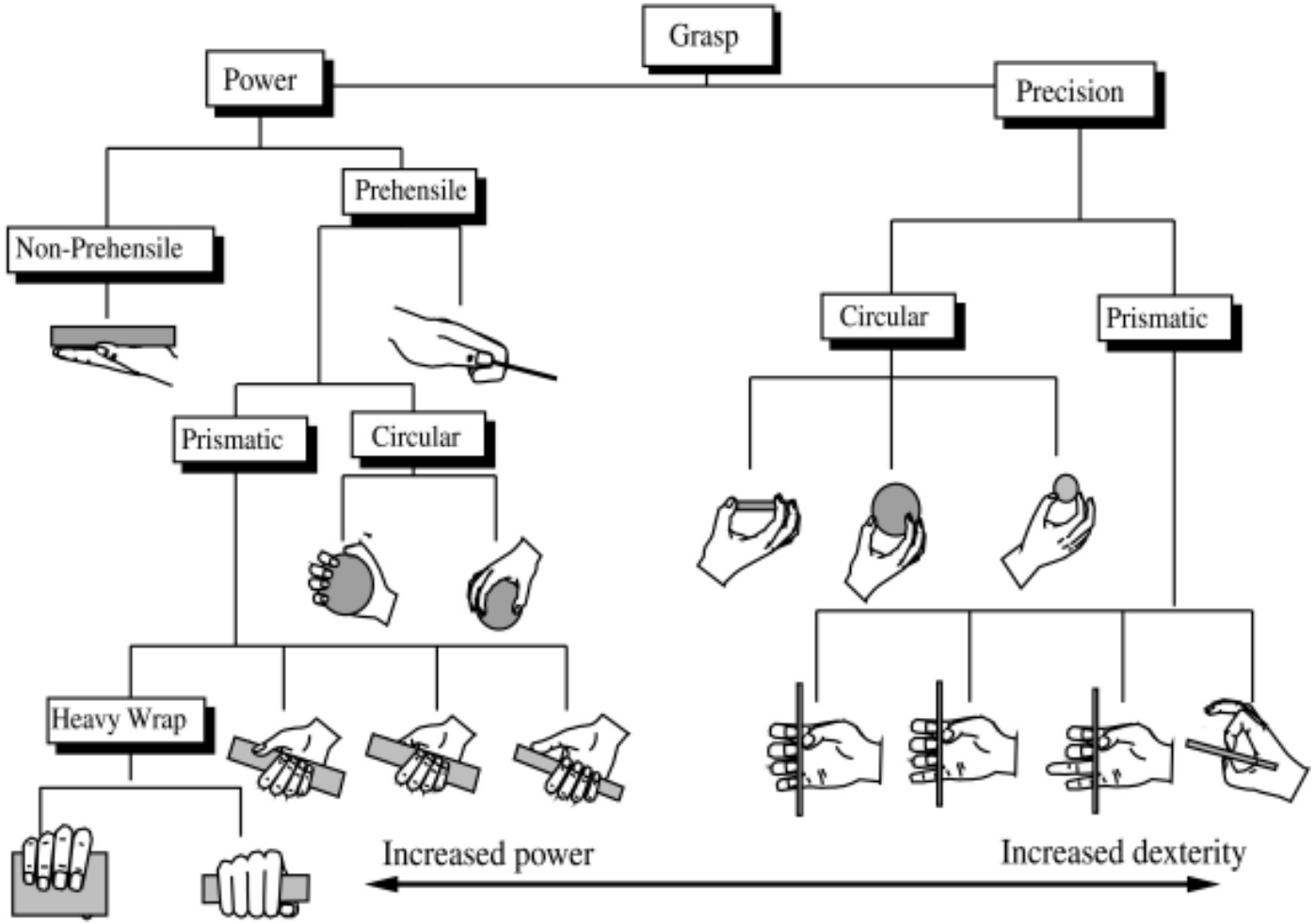

Human grasping configurations (*from [Burdea& Coiffet 2003]*)

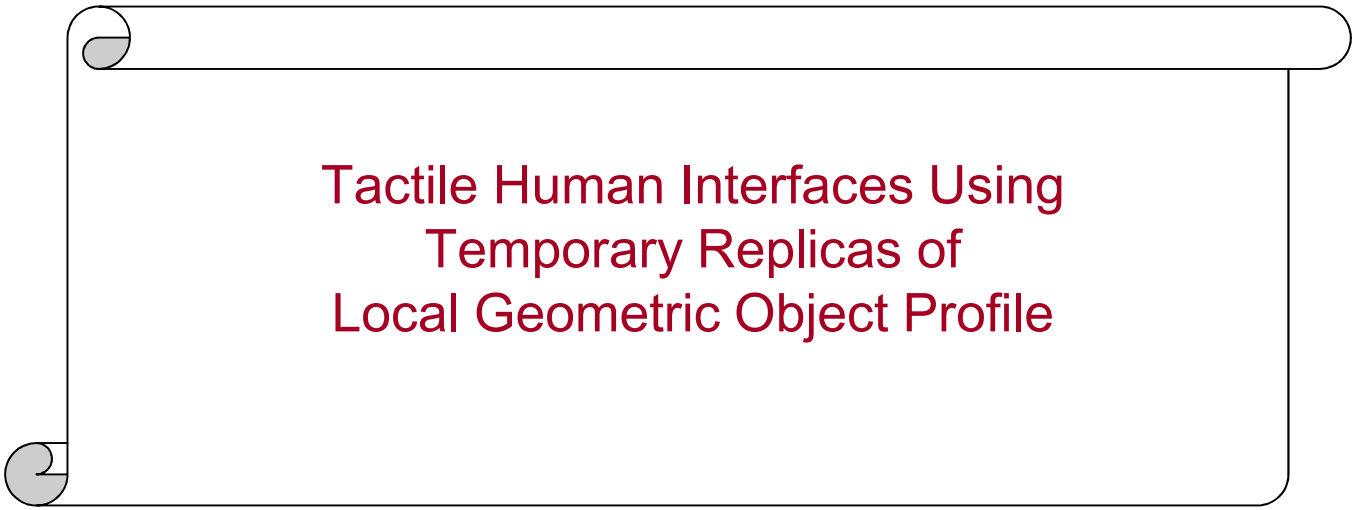
Tactile Human Interfaces Using
Temporary Replicas of
Local Geometric Object Profile

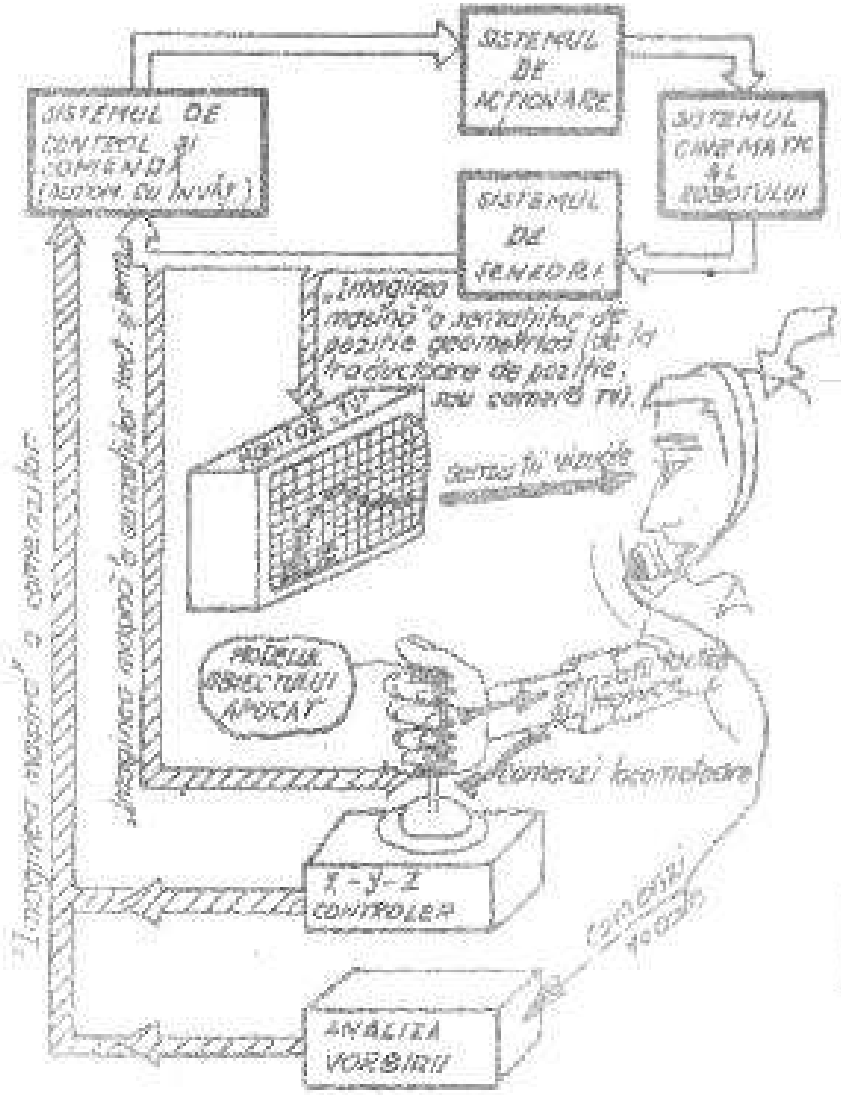

System architecture

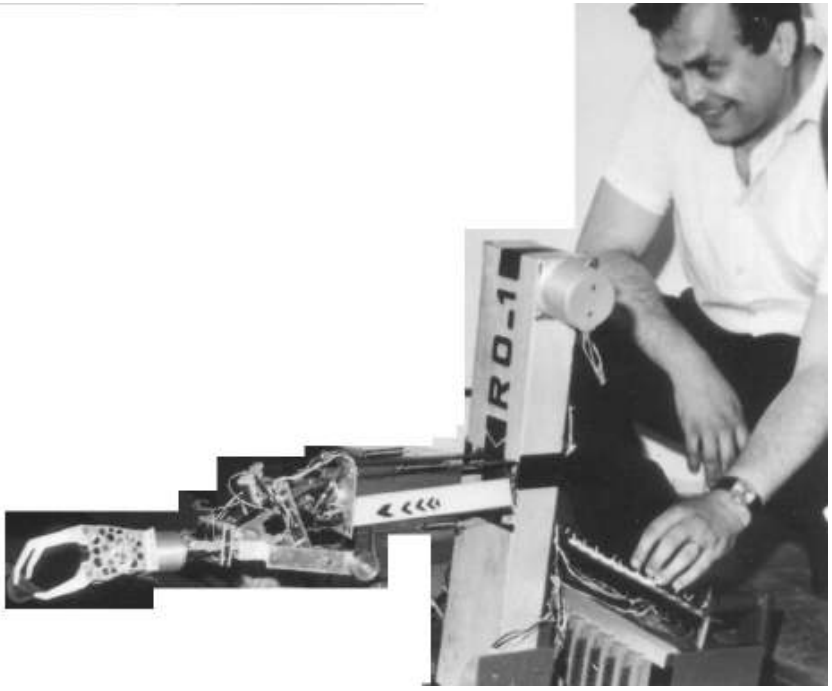

Robot arm with tendon driven compliant wrist

Video and Haptic Telerobotic System (from [E.M. Petriu, D.C. Petriu, V. Cretu, "Control System for an Interactive Programmable Robot," *Proc. CNETAC Nat. Conf. Electronics, Telecommunications, Control, and Computers*, pp. 227-235, Bucharest, Romania, Nov. 1982]).

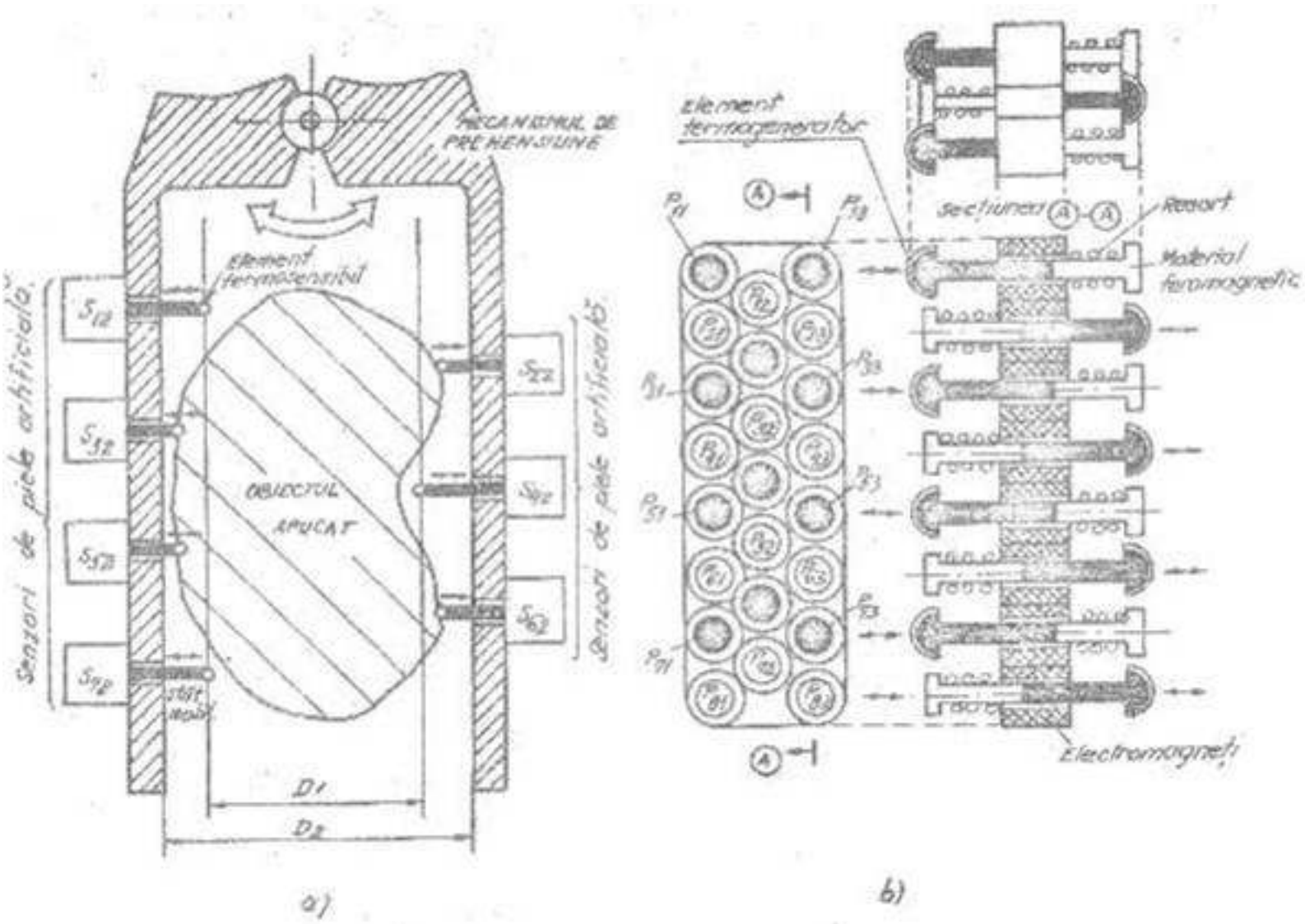

Video and Haptic Telerobotic System: (a) the tactile probe , and (b) the tactile human feedback (from [E.M. Petriu, D.C. Petriu, V. Cretu, "Control System for an Interactive Programmable Robot," *Proc. CNETAC Nat. Conf. Electronics, Telecommunications, Control, and Computers*, pp. 227-235, Bucharest, Romania, Nov. 1982.])

Model-based telepresence control of a robot (early 90s)

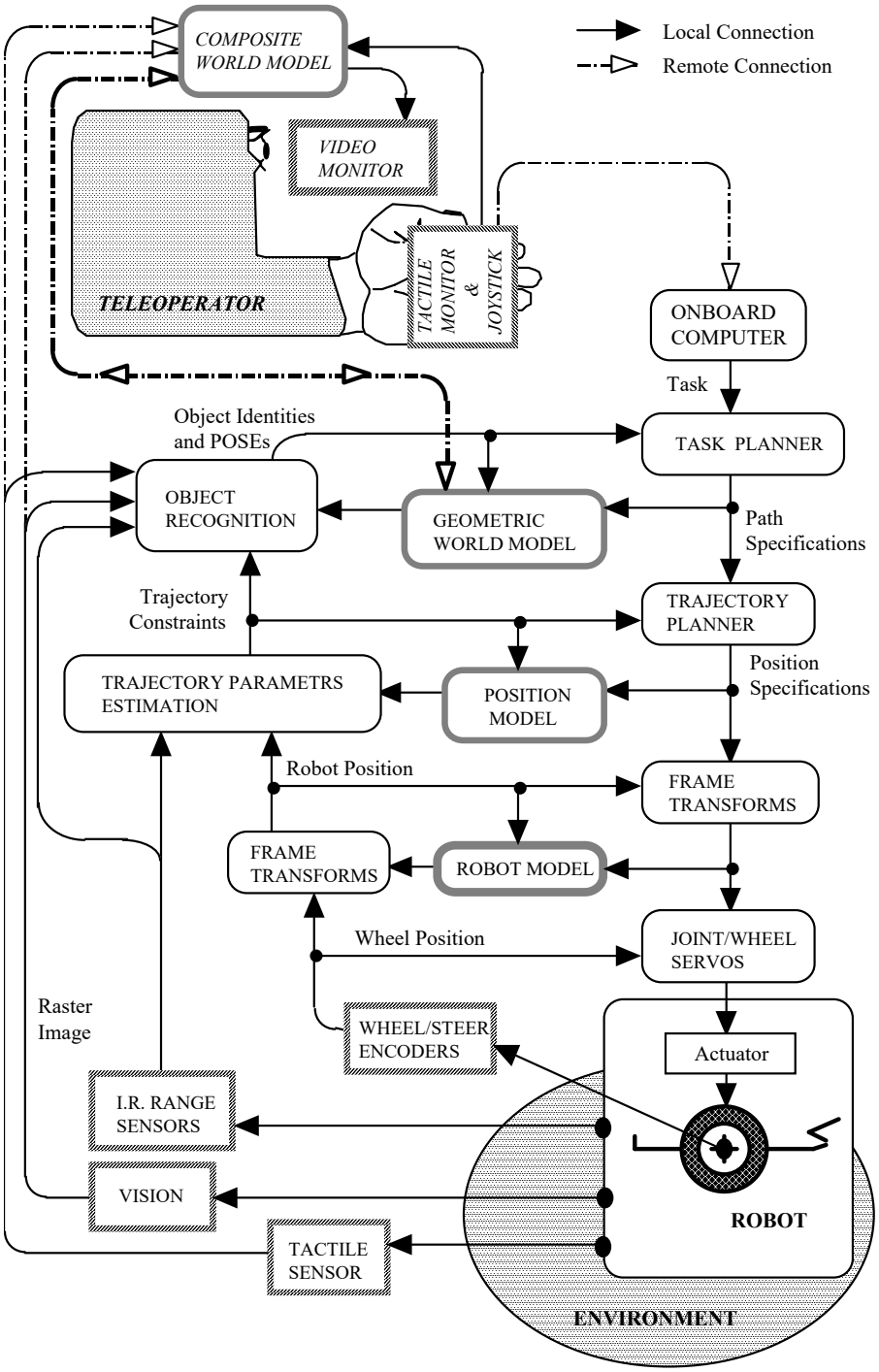

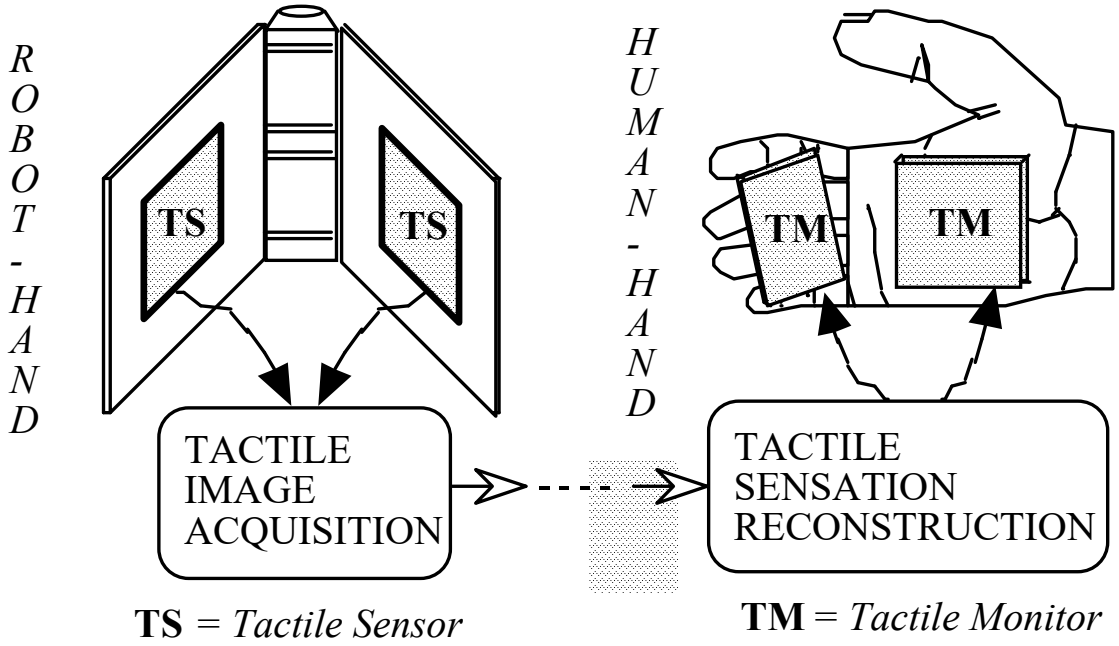

A tactile monitor placed on the operator's palm allows the human teleoperator to virtually feel by touch the object profile measured by the tactile sensors placed in the jaws of the robot gripper (from [E.M. Petriu, W.S. McMath, "Tactile Operator Interface for Semi-autonomous Robotic Applications," *Proc.Int. Symposium on Artificial Intell. Robotics Automat. in Space, i-SAIRS'92*, pp.77-82, Toulouse, France, 1992.])

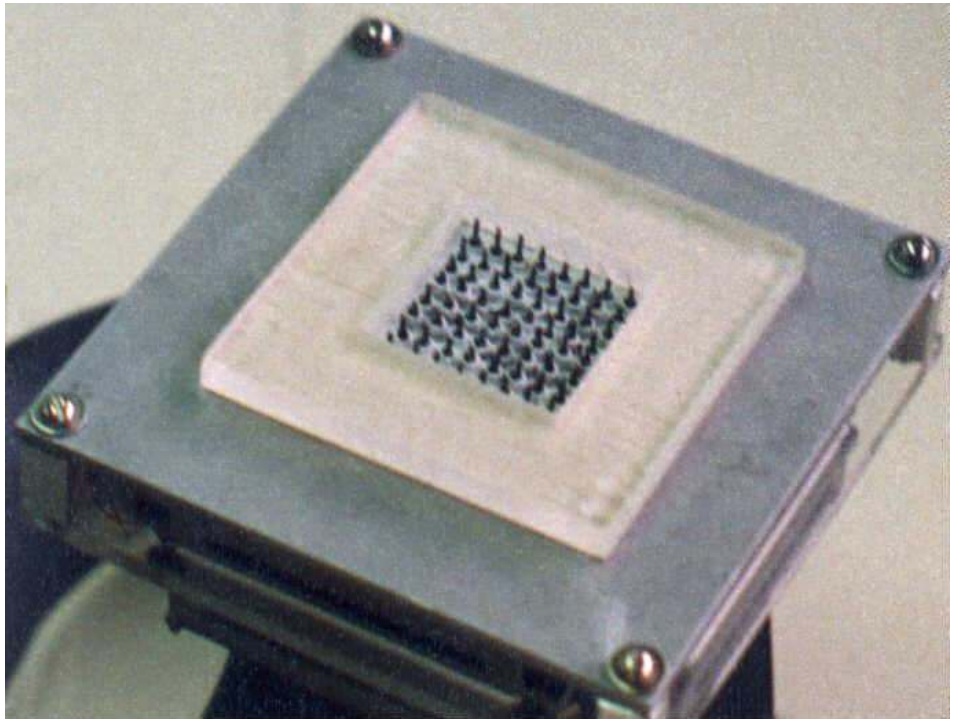

Cutaneous tactile monitor developed at the University of Ottawa in the early 90s. It consists of an 8-by-8 array of electromagnetic vibrotactile stimulators. The active area is 6.5 cm2 (same as the tactile sensor).

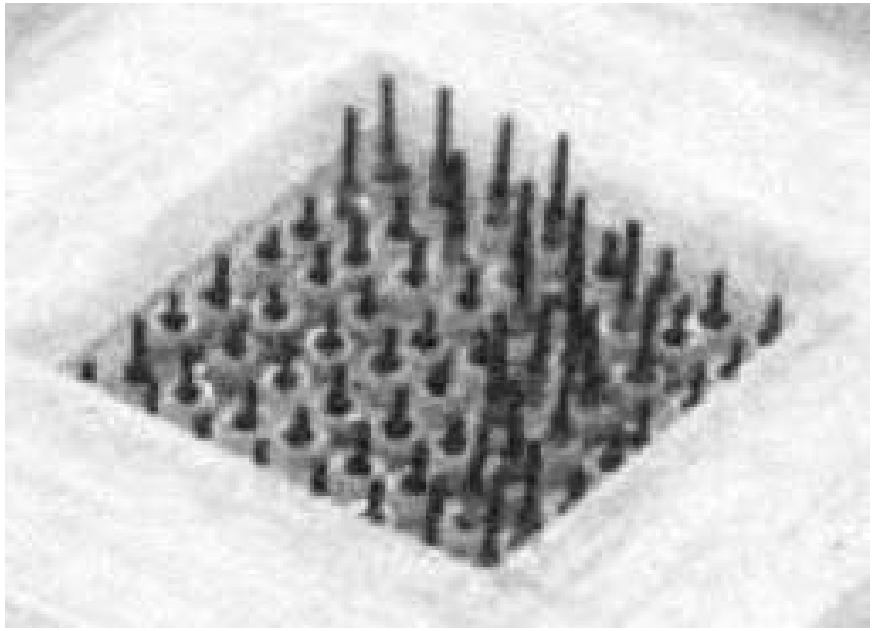

Each stimulator corresponds to a 2-by-2 window in the tactile sensor array. The vibrotactile stimulators are used as binary devices that are activated when at least two of the corresponding *taxels* (tactile elements) in the tactile sensor array window are "on". The figure shows a curved edge tactile feedback .

Maximum and Sustained Force Exertion

(*from [Burdea & Coiffet 2003]*)

- maximum force exerted during “power” grasp averages 400 N (male) and 225 N (female);
- function of body location, force output grows from 50 N at PIP finger joint, to 100 N at shoulder;
- sustained force feedback is much smaller than maximum, owing to fatigue and pain

Haptic Feedback Actuator Requirements
(*from [Burdea & Coiffet 2003]*)

- need to maximize power/weight ratio;
- need to have high power/volume ratio;
- need to have high bandwidth;
- need to have high dynamic range (fidelity);
- need to be safe for the user

⇨ None of the current actuator technology satisfies all these requirements.

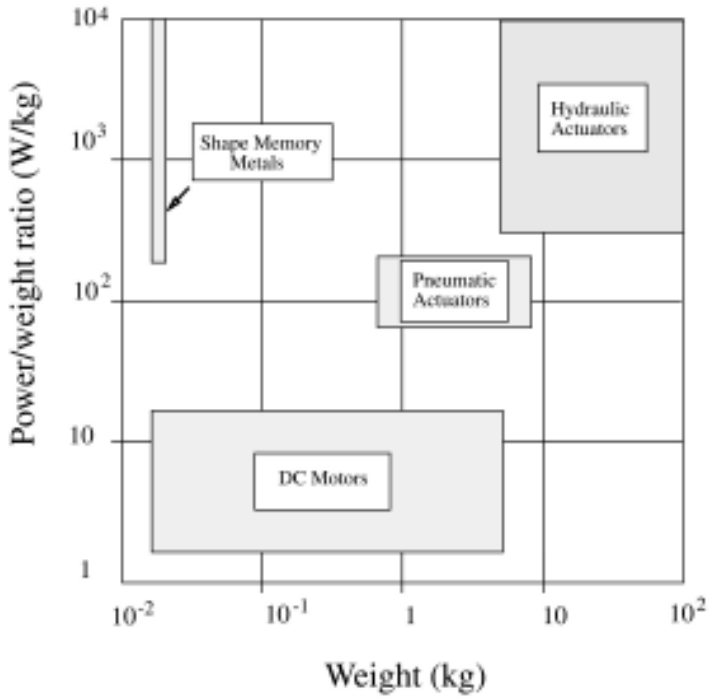

Actuator comparison based on P/W ratio (*from [Burdea & Coiffet 2003]*)

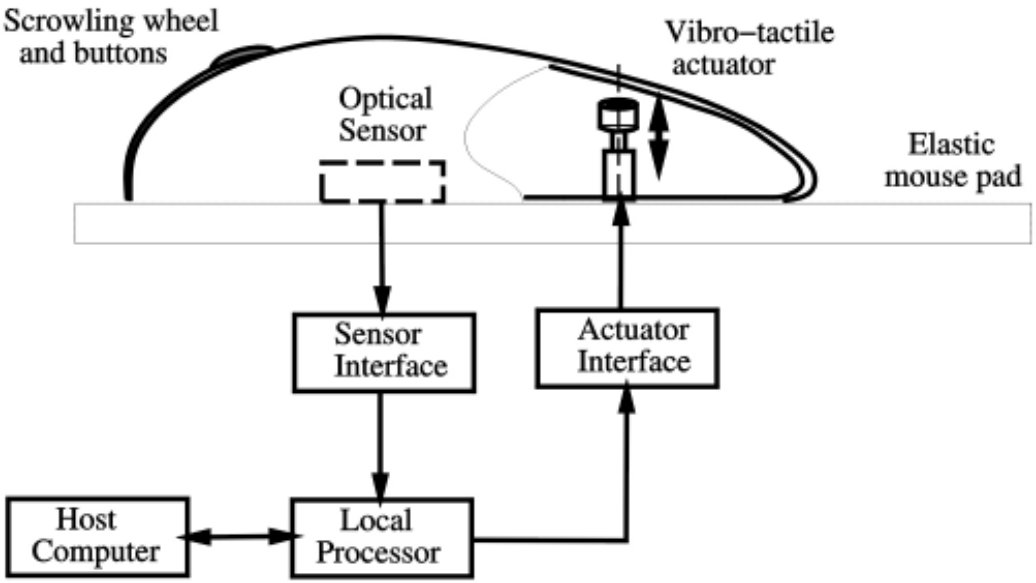

Logitech iFeel Mouse (0-125 Hz).

Immersionn_3D Interaction <http://www.immersion.com/>

CyberGlove®

CyberTouch™

CyberGrasp™

CyberForce®

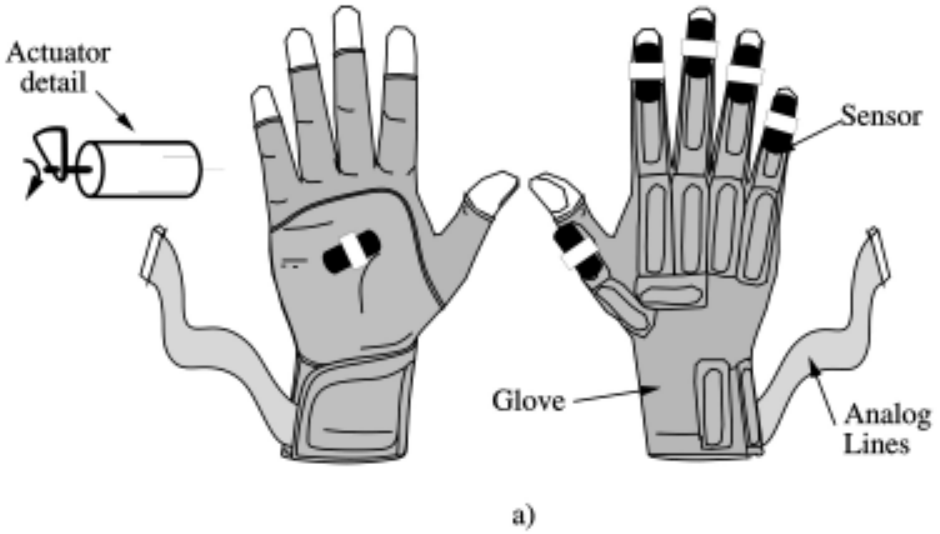

a)

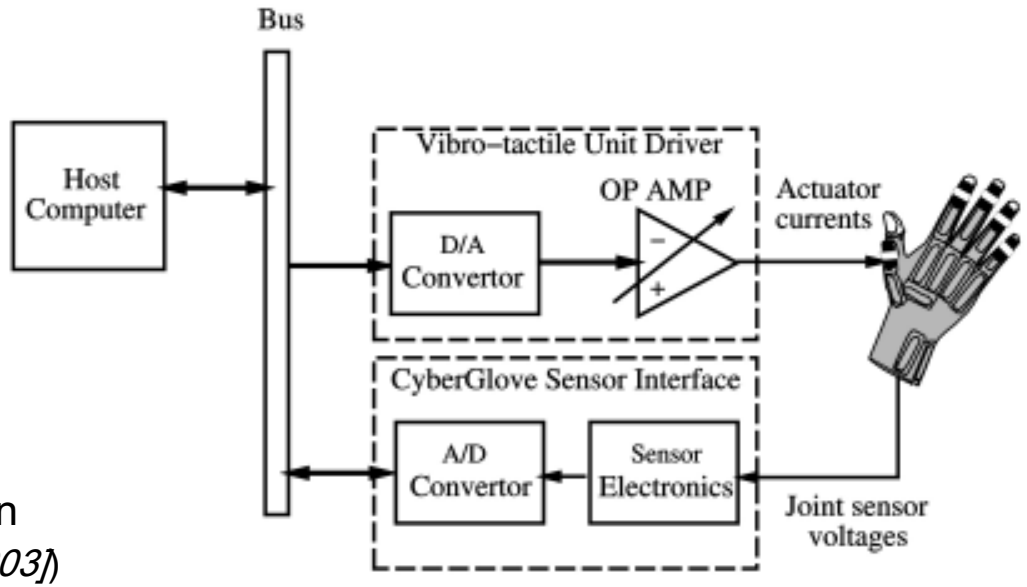

b)

CyberTouch Glove construction Details (*from [Burdea & Coiffet 2003]*)

Performance comparison of various sensing gloves *[Burdea& Coiffet 2003]*

Table 2.3 Performance comparison of various sensing gloves

Specs	Pinch Glove	5DT Glove	DidjiGlove	CyberGlove
Number Sensors	7/glove (two gloves)	5 or 14 /glove (one glove)	10/glove (two gloves)	18 or 22/glove (one glove)
Sensor type	electrical	fiberoptic	capacitive	strain gauge
Records /sec	??	100 (5DT 5W) 200 (5DT 5)	70	150 (unfiltered) 112 (filtered)
Sensor resolution	1 bit (two points)	8 bit (256 points)	10 bit (1,024 points)	0.5^o
Comm. rates	wired (19.2 kb)	wireless (9.600 kb) wired (19.2 kb)	wired (19.2 kb)	wired (115 kb)
Wrist sensors	none	pitch (5DT 5 model)	none	pitch and yaw

Immersionn_3D Interaction <http://www.immersion.com/>

CyberGlove®

- uses 18-22 linear sensors – electrical strain gauges;
- angles are obtained by measuring voltages on a Wheastone bridge;
- 112 gestures/sec “filtered”.
- sensor resolution 0.5 degrees, but errors accumulate to the fingertip (open kinematic chain);
- sensor repeatability 1 degree
- needs calibration when put on the hand

6 individually controlled vibrotactile actuators

0-125 Hz frequency;
1.2 N amplitude at 125 Hz.

CyberTouch Glove (Virtex) (*from [Burdea & Coiffet 2003]*)

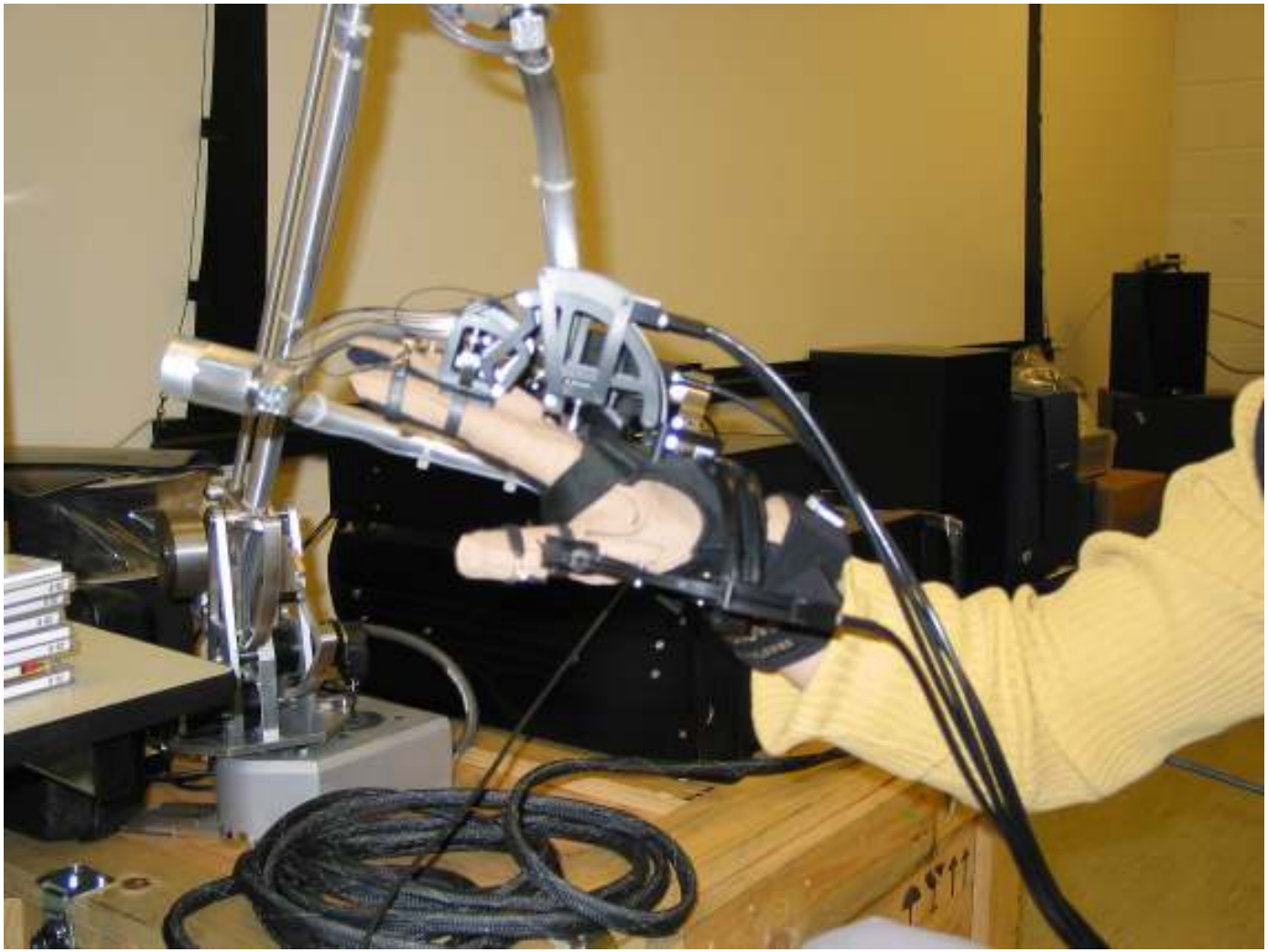

Commercial “Virtual Hand Toolkit for CyberGlove/Grasp” providing the kinesthetic human feedback interface

Tactile Human Interfaces Using Permanent Replicas of Whole Typical Objects

There are many telemanipulation applications which involve the **handling of a limited set of objects, usually tools**.

***Stylus* type tools** such as *pens, surgeon knifes, screwdrivers, probing rods*, etc are frequently used in dexterous manipulation applications.

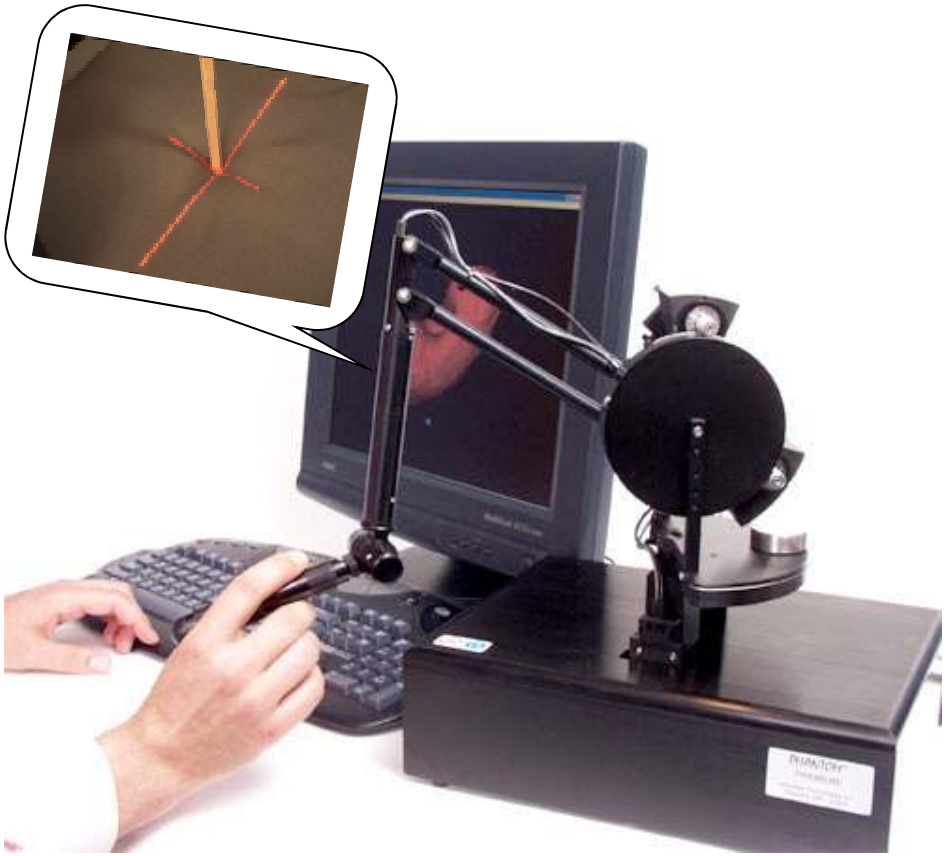

A desktop *hapto-visual human interface* allows a human teleoperator to experience the haptic feeling profiles at the point of contact as well as to see the image of a larger area around the point of contact on the explored object as captured by a video camera mounted on the robot manipulator. It includes a *PHANTOM® 6DOF* haptic device representing the **handheld replica of the probing rode** that provides the haptic feedback consisting of the 3D geometric coordinates of the point of contact measured by the laser range finder systemand the force vector and torque components measured by the 6 DOF force-torque sensor at the point of contact.

Robotic Tactile Recognition of Pseudo-Random Encoded 3D Objects

E.M. Petriu, S.K.S. Yeung, S.R. Das, A.M. Cretu, H.J.W. Spoelder, "Robotic Tactile Recognition of Pseudorandom Encoded Objects, IEEE Trans. Instrum. Meas., Vol.53, No.5, pp.1425-1432, 2004.

Pseudo-Random Binary Encoding provide a practical solution allowing absolute position recovery with any desired *n*-bit resolution while employing only one binary track, regardless of the value of *n*.

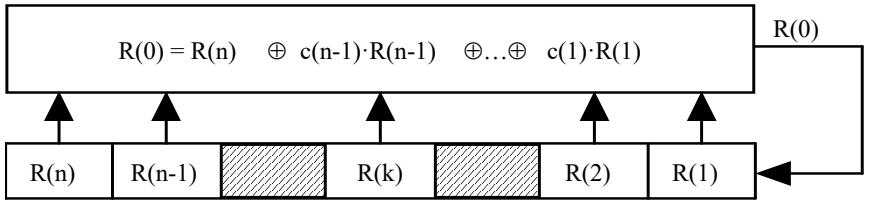

Table 1 Feedback equations for PRBS generation

Shift register length *n*	Feedback for direct PRBS R(0)= R(n) ⊕ c(n-1)·R(n-1) ⊕…⊕ c(1)·R(1)	Feedback for reverse PRBS R(n+1)= R(1) ⊕ b(2)·R(2) ⊕…⊕ b(n)·R(n)
4	R(0) = R(4) ⊕ R(1)	R(5) = R(1) ⊕ R(2)
5	R(0) = R(5) ⊕ R(2)	R(6) = R(1) ⊕ R(3)
6	R(0) = R(6) ⊕ R(1)	R(7) = R(1) ⊕ R(2)
7	R(0) = R(7) ⊕ R(3)	R(8) = R(1) ⊕ R(4)
8	R(0) = R(8) ⊕ R(4) ⊕ R(3) ⊕ R(2)	R(9) = R(1) ⊕ R(3) ⊕ R(4) ⊕ R(5)
9	R(0) = R(9) ⊕ R(4)	R(10) = R(1) ⊕ R(5)
10	R(0) = R(10) ⊕ R(3)	R(11) = R(1) ⊕ R(4)

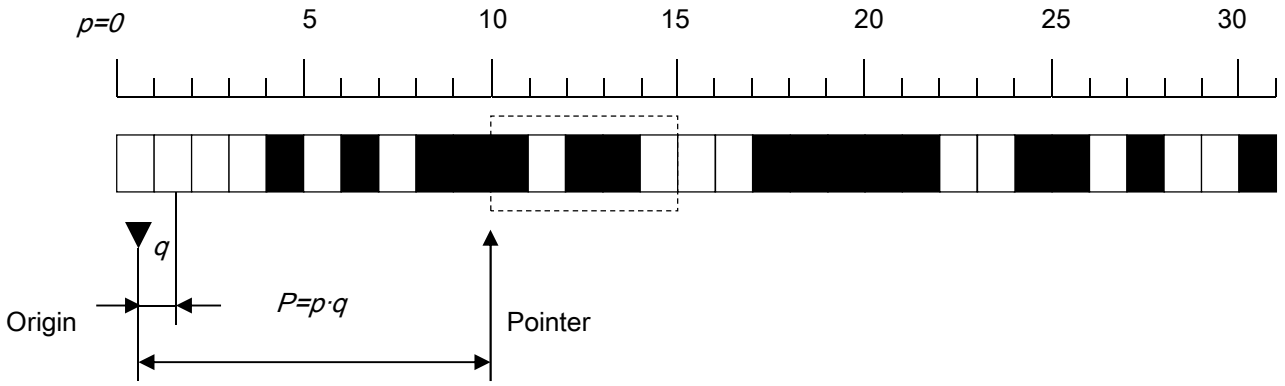

A 31-bit term PRBS: 0, 0, 0, 0, 1, 0, 1, 0, 1, 1, 1, 0, 1, 1, 0, 0, 0, 1, 1,1, 1, 1, 0, 0, 1, 1, 0,1, 0, 0, 1, generated by a 5-bit shift register. The 5-bit *n*-tuples seen through a window sliding over this PRBS are unique and represent a 1-bit wide absolute position code.

n	q=3	q=4	q=8	q=9
2	x^2+x+2	x^2+x+A x^2+Ax+A	x^2+x+A	
3	x^3+2x+1	$x^3+^{x2+}x+A$	x^3+x+A	x^3+x+A
4	x^4+x+2	$x^+{+}x^2+Ax+A^2$	x^4+x+A^3	x^4+x+A^5
5	x^5+2x+1	x^5+x+A $x^5+x^2+x+A^3$	x^5+x^2+A	
6	x^6+x+2	x^6+x^2+x+A	x^6+x+A	x^6+x^2+Ax+A
7	$x^7+x^6+x^4+1$	$x^7+x^2+Ax+A^2$	$x^7+x^2+Ax+A^3$	x^7+x+A
8	x^8+x^5+2	x^8+x^3+x+A		
9	$x^9+x^7+x^5+1$	x^9+x^2+x+A		
10	$x^{10}+x^9+x^7+2$	$x^{10}+x^3+A(x^2+x+1)$		

The following relations apply:

for GF(4)= GF(2^2): $A^2+A+1=0$, $A^2=A+1$, and $A^3=1$

for GF(8)= GF(2^3): $A^3+A+1=0$, $A^3=A+1$, $A^4=A^2+A$, $A^5=A^2+A+1$, $A^6=A^2+1$, and $A^{7=}1$

for GF(9)= GF(3^2): $A^2+2A+2=0$, $A^2=A+1$, $A^3=2A+1$, $A^4=2$, $A^5=2A$, $A^6=2A+2$, $A^7=A+2$, and $A^8=1$

According to the PRMVS window property any q-valued contents observed through a n-position window sliding over the PRMVS is unique and fully identifies the current position of the window.

$$
\begin{array}{ccccccccccccccccc}
0 & A & 1 & A^2 & A & A^2 & A^2 & A^2 & 1 & 1 & A^2 & A^2 & A^2 & A & A^2 & 1 & A \\
0 & 0 & 1 & A^2 & A^2 & A & 1 & 0 & A^2 & A^2 & 0 & 1 & A & A^2 & A^2 & 1 & 0 \\
0 & A^2 & 0 & 0 & A & A & A^2 & 1 & A^2 & A^2 & 1 & A^2 & A & A & 0 & 0 & A^2 \\
0 & 1 & A & 1 & A & 0 & A^2 & A & 0 & 0 & A & A^2 & 0 & A & 1 & A & 1 \\
0 & A^2 & A^2 & A & 0 & A^2 & 0 & 1 & 1 & 1 & 1 & 0 & A^2 & 0 & A & A^2 & A^2 \\
0 & A^2 & A & 1 & A2 & 1 & 1 & 1 & A & A & 1 & 1 & 1 & A^2 & 1 & A & A^2 \\
0 & 0 & A & 1 & 1 & A^2 & A & 0 & 1 & 1 & 0 & A & A^2 & 1 & 1 & A & 0 \\
0 & 1 & 0 & 0 & A^2 & A^2 & 1 & A & 1 & 1 & A & 1 & A^2 & A^2 & 0 & 0 & 1 \\
0 & A & A^2 & A & A^2 & 0 & 1 & A^2 & 0 & 0 & A^2 & 1 & 0 & A^2 & A & A^2 & A \\
0 & 1 & 1 & A^2 & 0 & 1 & 0 & A & A & A & A & 0 & 1 & 0 & A^2 & 1 & 1 \\
0 & 1 & A^2 & A & 1 & A & A & A & A^2 & A^2 & A & A & A & 1 & A & A^2 & 1 \\
0 & 0 & A^2 & A & A & 1 & A^2 & 0 & A & A & 0 & A^2 & 1 & A & A & A^2 & 0 \\
0 & A & 0 & 0 & 1 & 1 & A & A^2 & A & A & A^2 & A & 1 & 1 & 0 & 0 & A \\
0 & A^2 & 1 & A^2 & 1 & 0 & A & 1 & 0 & 0 & 1 & A & 0 & 1 & A^2 & 1 & A^2 \\
0 & A & A & 1 & 0 & A & 0 & A^2 & A^2 & A^2 & A^2 & 0 & A & 0 & & & 1 & A & A
\end{array}
$$

15-by-17 PRA obtained by folding a 255 element PRS defined over GF(4), with q=4, n=4, k1=2, k2=2, n1= q^{k1}-1=15, and n2=(q^n-1)/n1=17

PRA code elements are Braille-like embossed on object surfaces: 3D object models are unfolded and mapped on the encoding pseudo-random array.

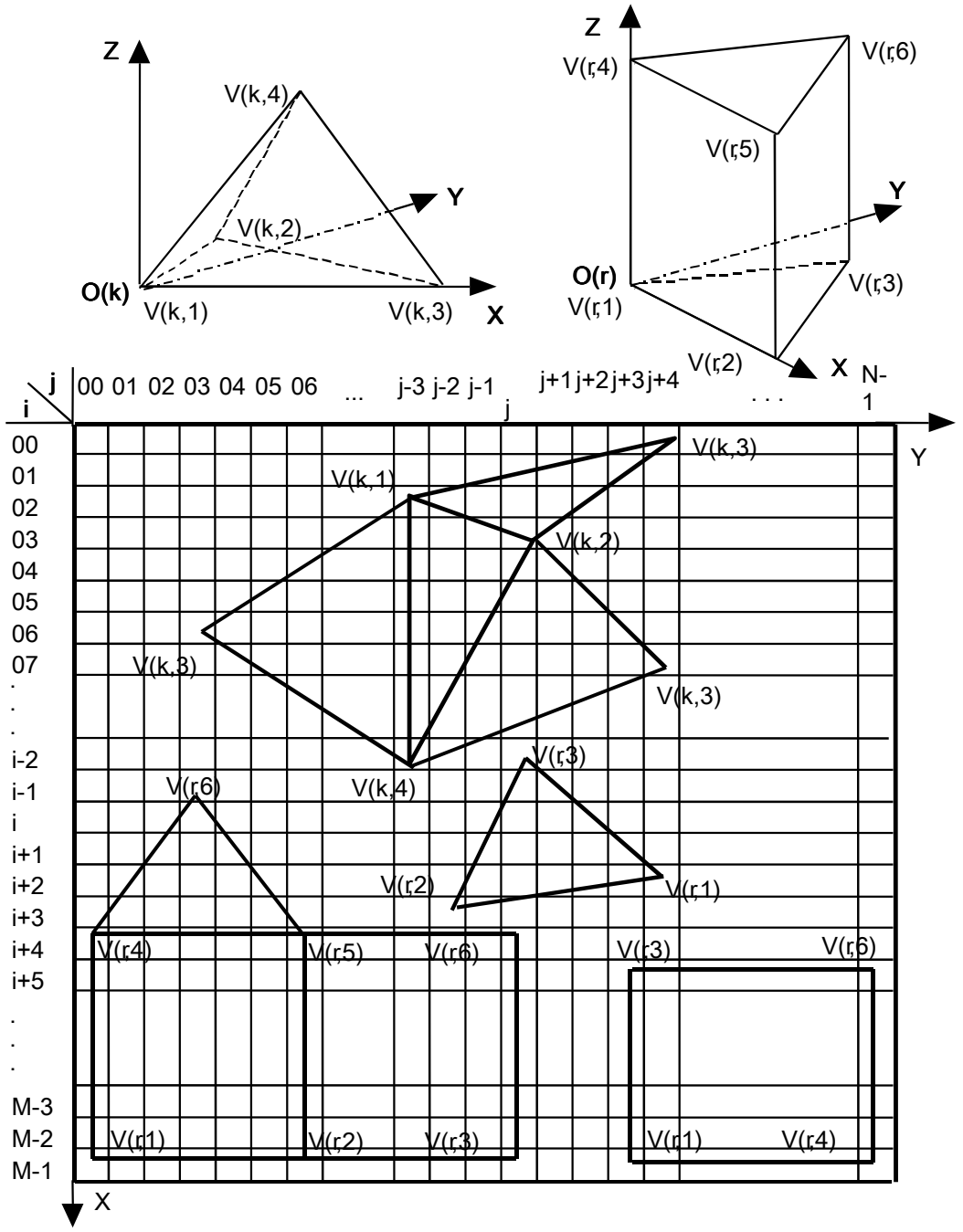

The shape of the embossed symbols is specially designed for easy tactile recognition. For an efficient pattern recognition, the particular shape of the binary symbols were selected in such a way to meet the following conditions:

(i) there is enough information at the symbol level to provide an immediate indication of the grid orientation;

(ii) the symbol recognition procedure is invariant to position, and orientation;

(iii) the symbols have a certain peculiarity so that other objects in the scene will not be mistaken for encoding symbols.

"0" "1"

The shape of the four code symbols for a PRA over GF(4) embossed on object's surface

"A" "A^2"

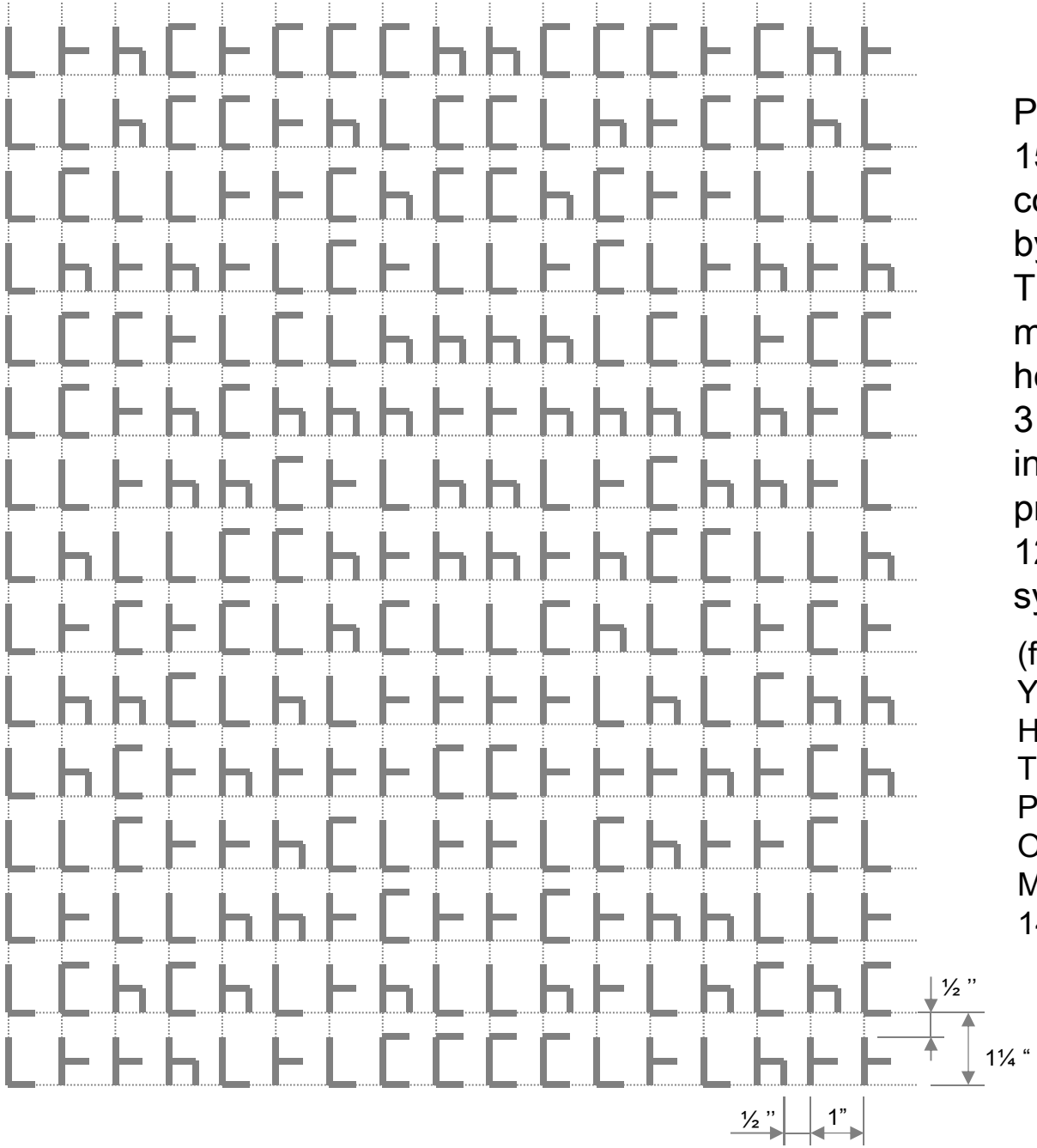

Physical layout of the 15-by-17 PRA with the code elements represented by four embossing symbols. The symbols are set 25.4 mm (1 inch) apart in the horizontal direction and 31.75 mm (1¼ inch) apart in the horizontal direction, providing a clear space of 12.7 mm (½ inch) between symbols in both directions.

(from [E.M. Petriu, S.K.S. Yeung, S.R. Das, A.M. Cretu, H.J.W. Spoelder, “Robotic Tactile Recognition of Pseudorandom Encoded Objects, IEEE Trans. Instrum. Meas., Vol.53, No.5, pp.1425-1432, 2004.])

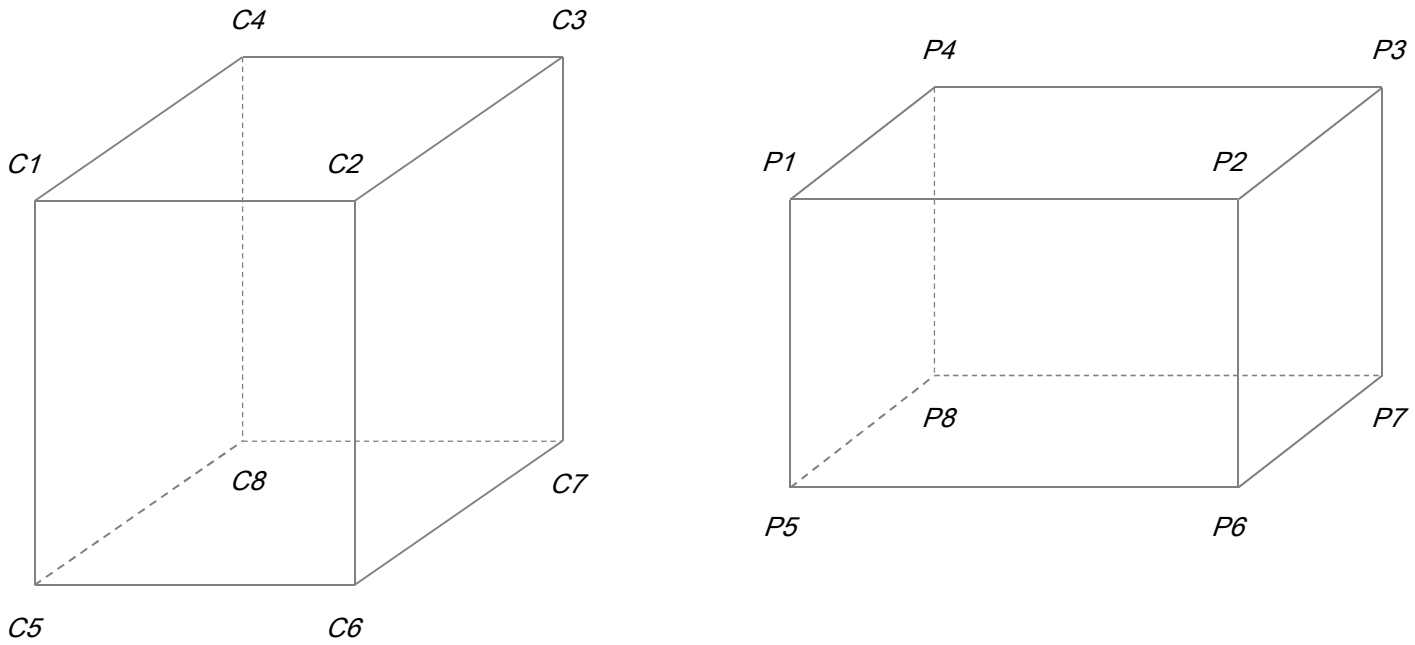

The vertex labeled models of two simple 3D objects

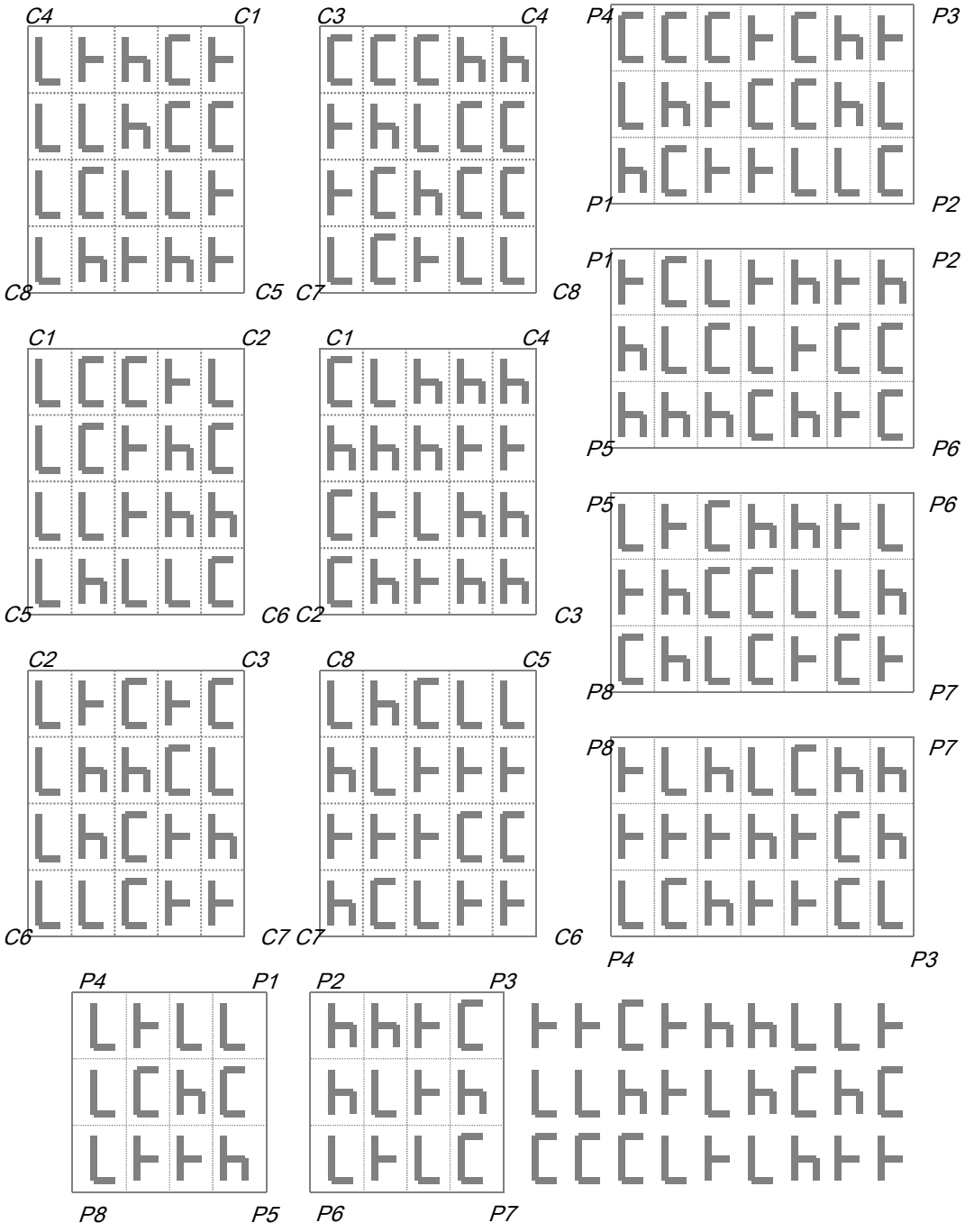

Mapping the embossed PRBA on the surfaces ofthe two 3D objects

(from [E.M. Petriu, S.K.S. Yeung, S.R. Das, A.M. Cretu, H.J.W. Spoelder, “Robotic Tactile Recognition of Pseudorandom Encoded Objects, IEEE Trans. Instrum. Meas., Vol.53, No.5, pp.1425-1432, 2004.])

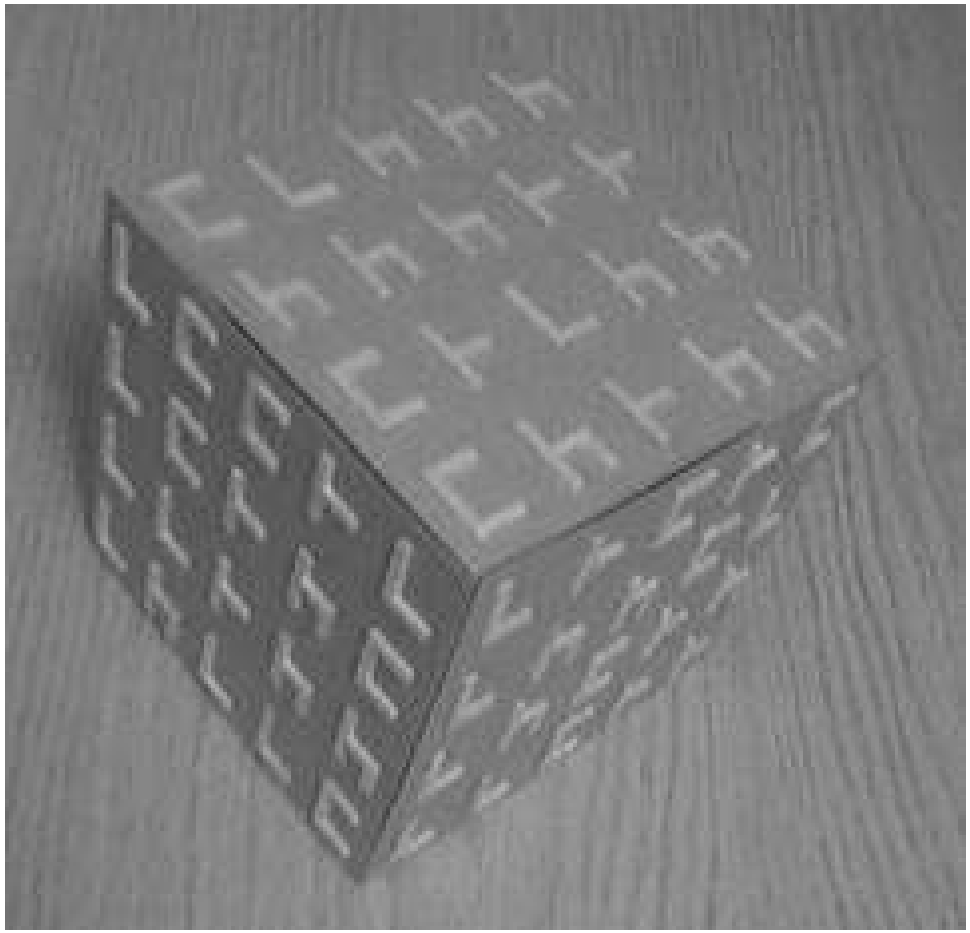

The PRA encoded cube.

(from [E.M. Petriu, S.K.S. Yeung, S.R. Das, A.M. Cretu, H.J.W. Spoelder, “Robotic Tactile Recognition of Pseudorandom Encoded Objects, IEEE Trans. Instrum. Meas., Vol.53, No.5, pp.1425-1432, 2004.])

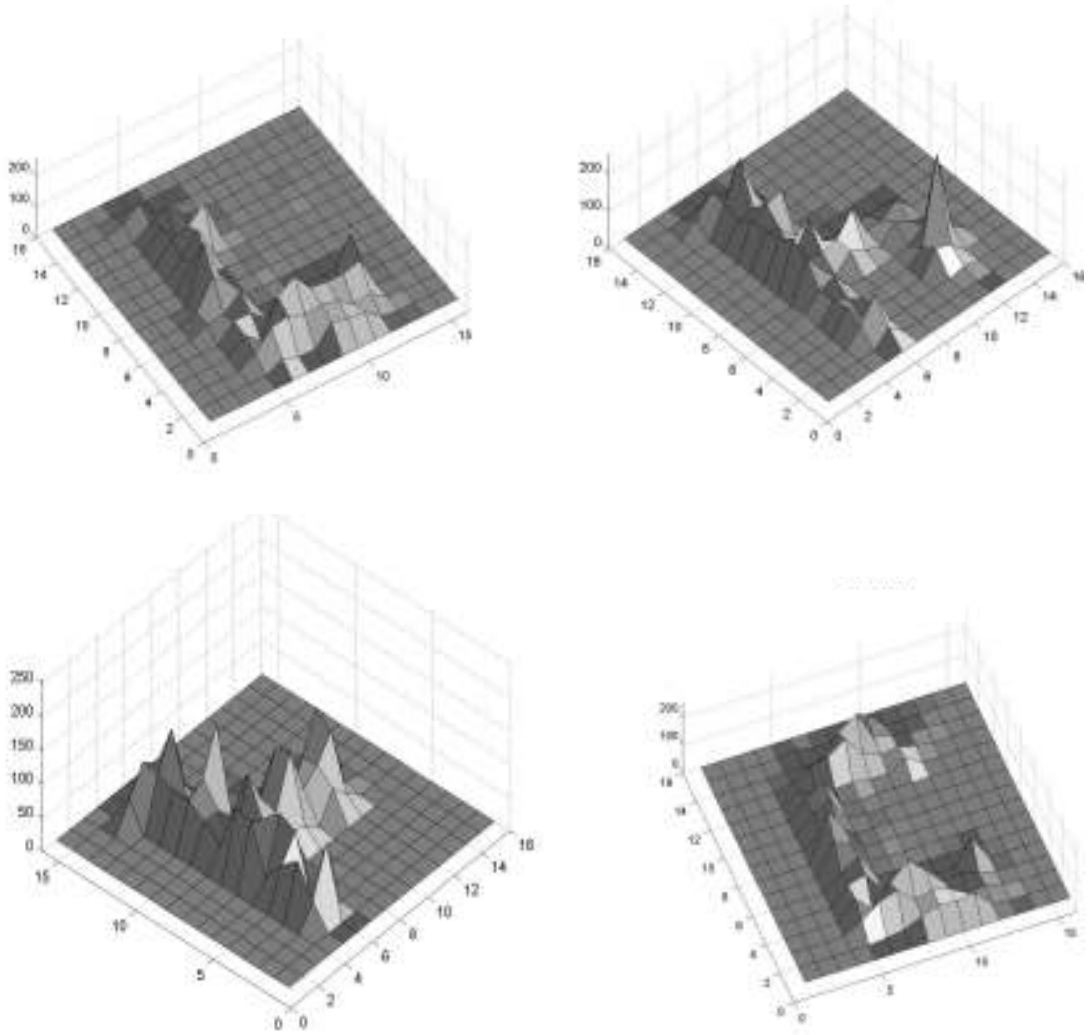

Tactile images of the four GF(4) symbols. The two rectangular axes on the horizontal plane in each image indicate the 2D node coordinates of the 16-by-16 tactile image. One unit on the vertical axis corresponds to 0.015875 mm (0.01/16 inch).

(from [E.M. Petriu, S.K.S. Yeung, S.R. Das, A.M. Cretu, H.J.W. Spoelder, “Robotic Tactile Recognition of Pseudorandom Encoded Objects, IEEE Trans. Instrum. Meas., Vol.53, No.5, pp.1425-1432, 2004.])

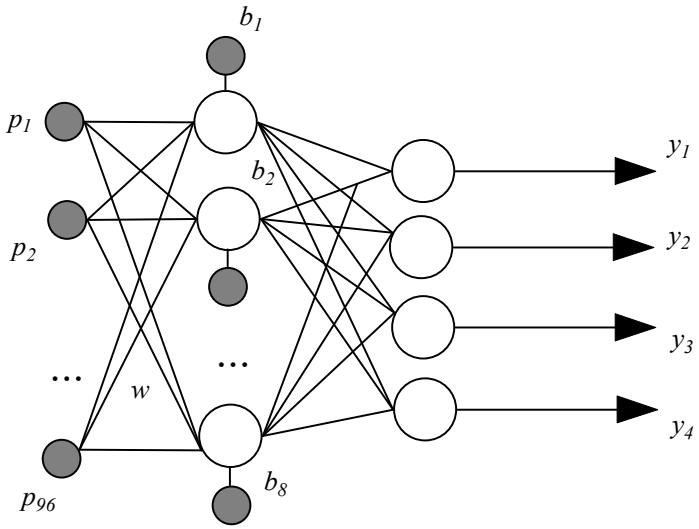

Two-layer feedforward NN architecture for the classification of the four GF(4) symbols.

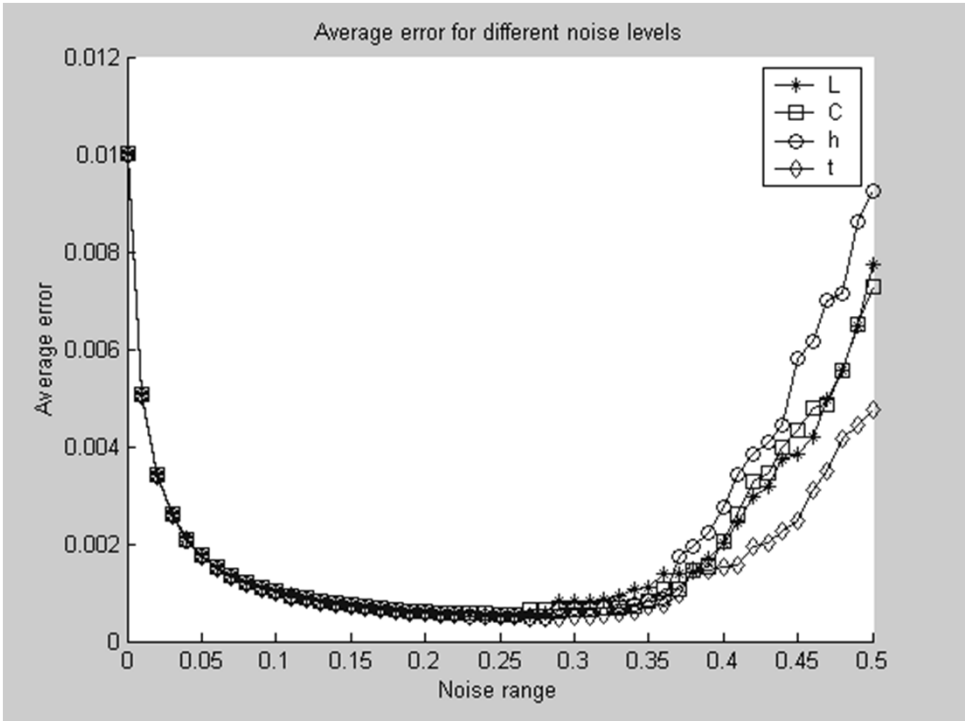

Average error rate for noise ranging between 0 and 0.5

(from [E.M. Petriu, S.K.S. Yeung, S.R. Das, A.M. Cretu, H.J.W. Spoelder, “Robotic Tactile Recognition of Pseudorandom Encoded Objects, IEEE Trans. Instrum. Meas., Vol.53, No.5, pp.1425-1432, 2004.])

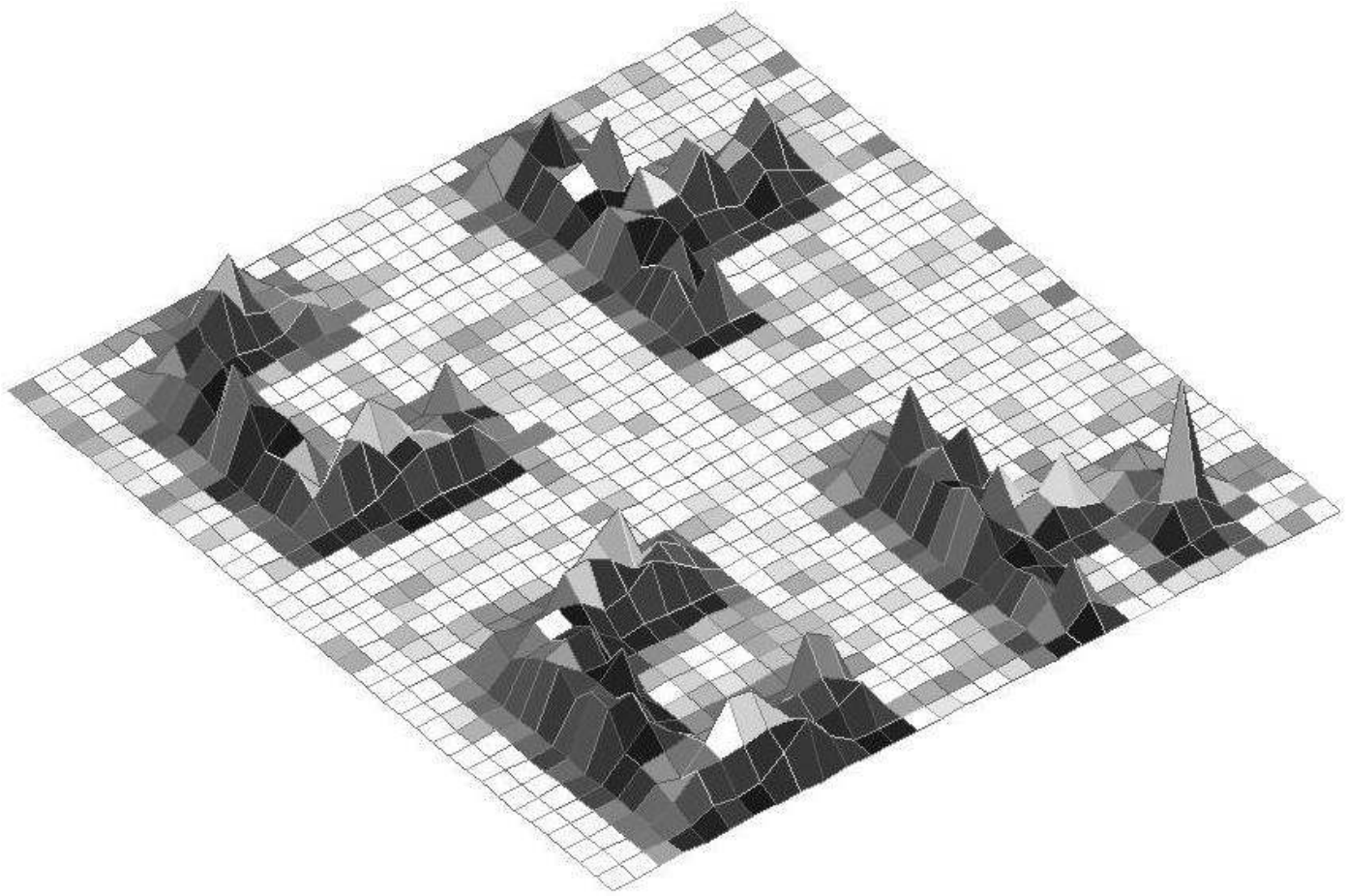

Composite tactile image of four symbols
on an encoded object surface

(from [E.M. Petriu, S.K.S. Yeung, S.R. Das, A.M. Cretu, H.J.W. Spoelder, “Robotic Tactile Recognition of Pseudorandom Encoded Objects, IEEE Trans. Instrum. Meas., Vol.53, No.5, pp.1425-1432, 2004.])

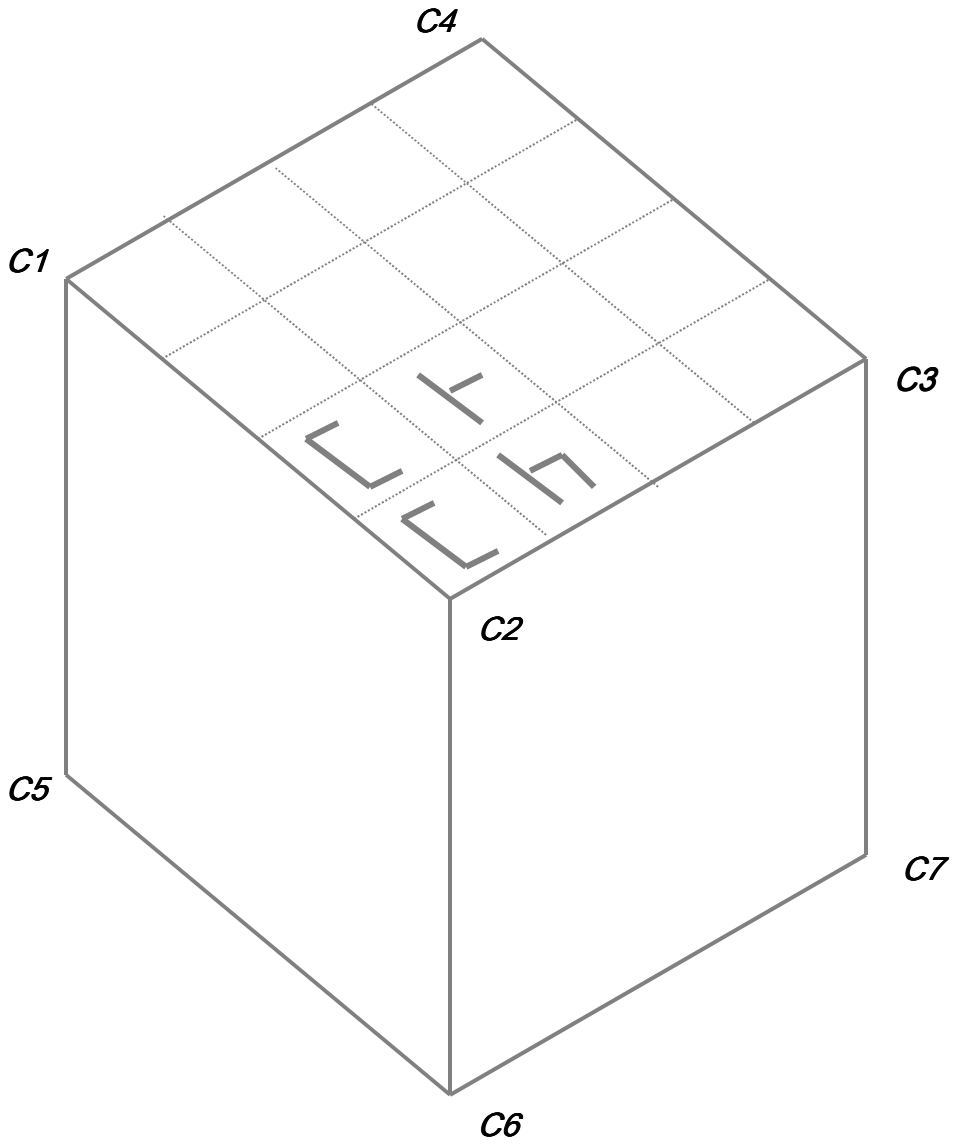

The four tactile recovered symbols are recognized, And their location is unequivocally identified on the face of one of the 3D objects, using the PRA window property.

(from [E.M. Petriu, S.K.S. Yeung, S.R. Das, A.M. Cretu, H.J.W. Spoelder, “Robotic Tactile Recognition of Pseudorandom Encoded Objects, IEEE Trans. Instrum. Meas., Vol.53, No.5, pp.1425-1432, 2004.])

Thank you !